A MATHEMATICAL MODEL OF THE SLEEP-WAKE CYCLE

A Thesis
Presented to
The Academic Faculty

by

Weiwei Yin

In Partial Fulfillment
of the Requirements for the Degree
Master in the
School of Bioengineering

Georgia Institute of Technology
May 2007

A MATHEMATICAL MODEL OF THE SLEEP-WAKE CYCLE

Approved by:

Dr. Eberhard O. Voit, Advisor
School of Wallace H. Coulter Dept. of Biomedical Engineering
Georgia Institute of Technology

Dr. Melissa Kemp
School of Wallace H. Coulter Dept. of Biomedical Engineering
Georgia Institute of Technology

Dr. Devanjan Sikder
School of Internal Medicine
UT Southwestern Medical Center

Date Approved: [April 4, 2007]

To Mom, Dad and my husband: without your support, I wouldn't be here

ACKNOWLEDGEMENTS

I would like to acknowledge Dr. Eberhard O. Voit, my advisor and mentor, for his invaluable guidance in my research. It would have been impossible for me to touch such an interesting research field and come this far without his willingness to give me a chance at the very beginning. I would also wish to thank I-Chun Chou, Gautam Goel, Zhen Qi, Jialiang Wu in the Biological Systems Analysis group for their great help both in my life and my research. Especially for I-Chun Chou and Gautam Goel, your suggestions and frequent discussions gave me a lot of new insights for my own research work. Finally, I would like to thank all my friends at Georgia Tech: thank you for letting me live so happily here.

TABLE OF CONTENTS

LIST OF TABLES

LIST OF FIGURES

SUMMARY

The daily sleep-wake cycle usually consists of three distinct states: wakefulness, non-rapid-eye-movement (NREM) and rapid-eye-movement (REM). The process of switching between different states is complex, but a common assumption is that it is regulated primarily by two processes (the circadian and the homeostatic process) via reciprocal interactions of several downstream neuron groups. These interactions not only result in often rapid transitions from one state to another, but also allow for a certain degree of bi-stability that locks the organism in a given state for some while before it switches back. In order to better understand how the behavioral states are regulated by different neuron groups, I describe how to use the S-system method for the development of a mathematical model consisting of two phases. The first phase covers the switch between wakefulness and sleep, which is controlled by the interactions between wake- and sleep-promoting neurons, whereas the second phase addresses the generation of NREM-REM alternation, which is believed to be regulated by REM-OFF and REM-ON neurons. In this set-up I interpret the circadian rhythm as external input and homeostatic regulation as a "feedback controller." Both open-loop and closed-loop forms of the two-phase model are investigated and implemented. Discharging activities of the corresponding neuron groups and the switches of behavioral states are shown in the simulation results, from which we can easily identify the basic roles of wake- and sleep-promoting neurons, REM-OFF and REM-ON neurons. The special regulatory function of the neuropeptide orexin is also tested by simulation.

CHAPTER 1

INTRODUCTION

The daily sleep-wake cycle usually consists of three distinct states: WAKE, NREM (non-rapid eye movement)/SWS (slow-wave sleep) and REM (rapid eye movement)/PS (paradoxical-sleep). These states are associated with different neurological profiles that differ in their electroencephalogram (EEG), electro-oculogram (EOG), electromyogram (EMG) and the degree of muscle tone [1]. The process of switching between different states is complex, but a common assumption is that it is primarily controlled by two processes via an interactive network of several downstream neuron groups. The first process is the "homeostatic process," which is an appetitive process determined by the amount of time awake. The longer the time spent awake, the greater the drive for sleep. Under normal circumstances, this process reaches the maximum level in the evening before the beginning of the sleep period. The second process is the "circadian process." It varies with a 24-hour periodicity and is independent of the amount of preceding sleep or wakefulness. These two processes together modulate the need for sleep and influence the balance between central alertness and sleepiness. This balance is linked to specific neuron groups, including wake-promoting neurons and sleep-promoting neurons, which could initiate reciprocal interactions and result in often rapid transitions from one state to another, but also allow for a certain degree of bi-stability that locks the organism in a given state for some while before it switches back. Lesions or loss of certain kinds of neurons may cause sleep disorders. For instance, recent experimental results [2-4]suggest that loss or mutation of the neuropeptide orexin or its receptor is intimately associated with a sleep disorder called narcolepsy. In this work, we will focus on the relationship between the behavioral states, two control processes and the underlying neuronal network.

Behavioral States

The electroencephalogram (EEG) [1] is a relatively simple measurement of brain activity that uses scalp electrodes to detect small signals primarily produced by cortical neurons. According to the frequency and amplitude of the recorded voltage, the EEG can be used to differentiate changes in wake and sleep stages. Usually, the low-voltage fast-frequency EEG pattern is characteristic of wakefulness and REM sleep. The high-voltage slow-wave EEG pattern indicates NREM sleep. The combined records of eye movement by EOG and muscle tone by EMG with EEG are sufficient to characterize wake and the main stages of sleep.

As sleep onset approaches, the low-voltage fast-frequency pattern of wake (Fig1.a) yields to stage 1 sleep and the EEG frequency begins to slow. Stage 1 sleep is followed by stages 2, 3 and 4, which are defined by the presence of high-amplitude, slow waves. Stages 3 and 4 are often grouped together using the term “slow-wave sleep” (NREM). As REM sleep begins, low-voltage fast-frequency waves then reappears on the EEG. The EEG pattern of REM sleep resembles that of active wakefulness, but it is further characterized by the presence of bursts of rapid eye movements and by loss of muscle tone in major muscle groups of the limbs, trunk and neck.

Each sleep stage typically and predictably progresses to the next stage during a night’s sleep (Fig1.b). The first REM episode, usually occurring at ~70 to 90 minutes after sleep onset, is short and, after the first episode, the sleep cycle repeats with the appearance of non-REM sleep. Then, ~90 minutes after the start of the first REM period, another REM sleep episode occurs. This rhythmic cycling persists throughout the night. The REM sleep cycle length is 90 minutes in humans, and the duration of each REM sleep episode after the first is ~30 minutes.

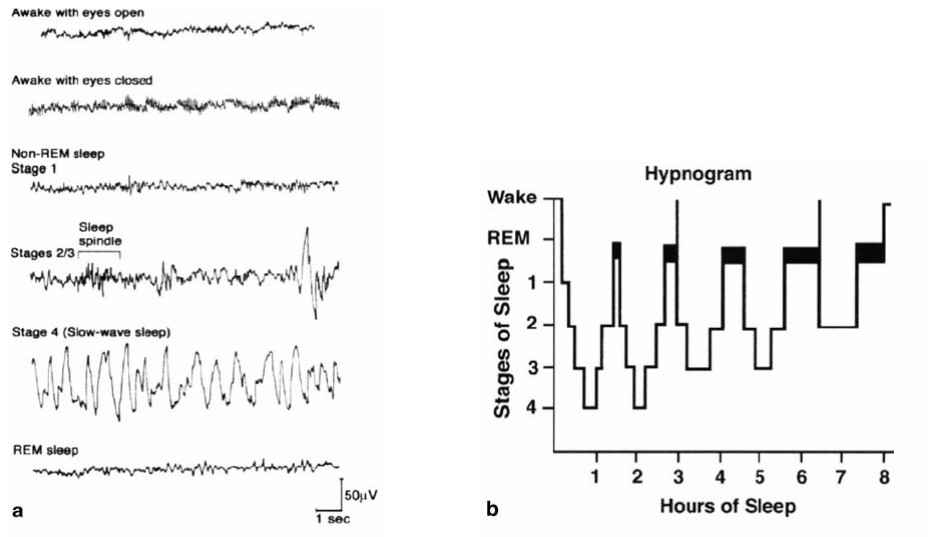

Fig. 1. Diagram of different behavioral states. (a) Electroencephalographic (EEG) patterns associated with wakefulness and the stages of sleep. (b) Hypnogram of the time course of sleep stages during a night's sleep in a healthy young adult.[5]

Neuron Groups

Neuron groups, mainly located in the basal forebrain, hypothalamus and brainstem, play an important role in regulating the sleep-wake cycle. They have different discharge profiles, neurotransmitters releasing and possible regulating functions. Pharmacological agonist/antagonist experiments and anatomical connectivity show evidence of putative afferents/efferent projecting in/out these neuron groups. We can simply separate them into two categories: the wake-promoting and the sleep-promoting group. The wake-promoting group mainly consists of monoamine-containing neurons and acetylcholine-containing neurons in brainstem and hypothalamus. The sleep-promoting neurons, mainly located in the preoptic areas, contain the inhibitory neurotransmitters GABA and/or galanin. Anatomical studies have provided evidence of bidirectional projections from these sleep-promoting neurons to all components of wake-promoting neurons. In the following, the details of these neurons are introduced. Fig. 2 shows how these neuron groups are distributed in the brain. The pathway of projections and the relationship between neuron groups and different behavioral states, which are also

illustrated to some extent in the same figure, will be introduced in detail later in this chapter. Abbreviated names of neurotransmitters are used as the name of the neuron group, *i.e.*, ACH, acetylcholine; NA, noradrenaline; 5-HT, serotonin; ORX, orexin/hyprocretin; HIS, histamine; GABA, gamma-aminobutyric acid and GLU, glutamine. Abbreviated names of neuron group locations that are frequently used in later chapters and figures are listed below: LC, the locus ceruleus; DR, dorsal raphe nucleus; TMN, the tuberomammillary nucleus; LHA, the lateral hypothalamus area; BF, the basal forebrain; POA, the preoptic area; VLPO, the ventrolateral preoptic area; eVLPO, the extended area of VLPO; MnPN, the median preoptic nucleus; SCN, suprachiasmatic nucleus; vSPZ, the ventral subparaventricular zone; DMH, dorsomedial nucleus. In the following chapters and figures, abbreviations given here won't be explained any more unless they have different meanings.

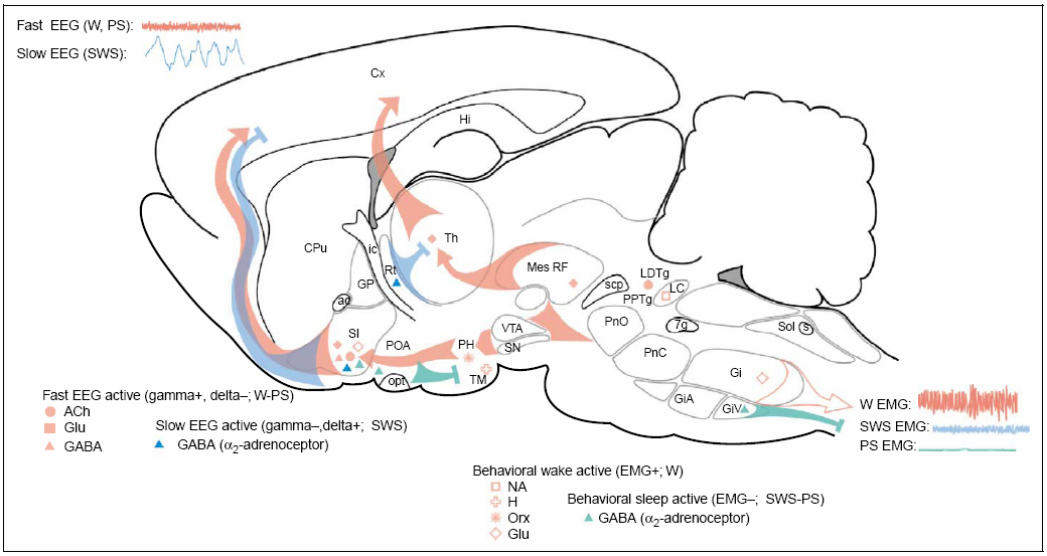

Fig. 2. The rat brain depicting neurons and their chemical neurotransmitters and pathways that influence either cortical activity or behavior throughout the sleep–wake cycle. The cortical EEG results of three states (wake, NREM, REM) are listed in upper left; the neck EMG results are listed in lower right. Neurons active in both WAKE and REM are indicated by filled pale red symbols; Neurons active only in WAKE are indicated by open pale red symbols; Neurons active with NREM (SWS) are blue triangle. Main abbreviations: LDTg, laterodorsal tegmental nucleus; PH, posterior hypothalamus; Th, thalamus; TM, tuberomammillary nuclei; VTA, ventral tegmental area. Please see [6] for other abbreviations.

Noradrenaline (NA)

Neurons in this group are mostly localized in the locus ceruleus (LC) of the pons [7]. Neuronal recording studies show that they have the highest firing rate during wakefulness, decrease their firing rate in NREM sleep and almost cease firing in REM sleep. They can be excited by ORX, ACH and HIS neurons [8, 9] and inhibited by 5HT and GABA in preoptic area [10]. As one hypothesis of REM sleep regulation indicates, these types of neurons not only act as wake-promoters, but also take part in the system permitting REM sleep by suppressing the cholinergic REM-ON neurons in brainstem[11].

Serotonin (5HT)

Neurons in this group are located in the dorsal raphe nucleus (DR) [7]. Like other monoamine-containing neurons, they are more active during wakefulness than sleep. Together with noradrenergic neurons, they have a role in regulating muscle tone and phase events of REM sleep [12, 13] , such as the generation of ponto-geniculo-occipital PGO waves. They can be excited by ORX [14], monoamine-containing neurons, such as HIS and NA and inhibited by GABA in brainstem and the preoptic area [7].

Histamine (HIS)

Neurons of this type are located in the tuberomammillary nucleus (TMN) of the posterior hypothalamus [7]. They have a similar discharge pattern as neurons in LC and DR. A recent study [15] shows that in cataplexy (a symptom associated with narcolepsy and loss of muscle tone during waking period), unlike noradrenergic and serotonergic neurons, histaminergic neurons are still active at a level similar to or greater than that in quiet waking, which indicates histamine-containing neurons may play a major role in maintenance of wakefulness. They can be excited by ORX and inhibited by GABA in the preoptic area [14, 16]. Although serotonin, histamine and noradrenaline cells normally

turn off during REM sleep, the fact that under some conditions, such as in cataplexy, these three cell groups don't cease activity together shows that they can be controlled individually by various GABA-containing cell populations.

Orexin (ORX)

Orexin (also called hypocretin)-containing neurons are distributed in a restricted region of perifornical region of the lateral hypothalamus [14, 17]. Though small in number, orexin neurons extend a widely projecting efferent system that innervates virtually the entire central nervous system. Particularly, orexin neurons activate a variety of ascending aminergic transmitter systems implicated in the regulation of arousal, including the noradrenergic, histaminergic, cholinergic, serotonergic and dopaminergic systems [18]. In addition, they are self-excited via local glutamate neurons [19]. A putative role of orexin-containing neurons is the maintenance of wakefulness and acting as a connection between sleep-wake regulation and energy homeostasis [14, 20, 21]. An activity study [22] has shown that orexin-containing neurons display relative low discharge levels in both REM and NREM sleep while high discharge rates in alert waking. However, discharge rates were not substantially elevated during quiet waking, suggesting that orexin neurotransmission is not only associated with waking *per se*. In this work, since I do not separate quiet waking and alert waking, I coarsely assume that orexin-containing neurons are active during the entire wake period while inactive during sleep periods.

Acetylcholine (ACH)

There are two main locations containing this type of neurons. One is the basal forebrain [23], where cholinergic neurons receive downstream projections from the brainstem activating system and posterior hypothalamus, and send upstream projections to cerebral cortex and thalamus. The other is the brainstem area, including the

laterodorsal tegmental nucleus (LDT), the pedunculopontine tegmental nucleus (PPT), the peri-LCα and the nucleus reticularis magnocellularis (NMC). An electrical activity study[24] of single cells in PPT has shown three dominant discharge patterns: REM-ON cells (more active during REM sleep than the other two states), WAKE-REM-ON cells (more active during both WAKE and REM sleep than NREM sleep), and State-Independent cells (not changing as a function of behavioral states). A putative role of this kind of neurons in brainstem comes from the reciprocal-interaction model [11] that cholinergic REM-ON neurons and monoaminergic REM-OFF neurons reciprocally interact with each other and result in the ultradian alternation of mammalian REM and NREM sleep. The mechanism and the network structure of brainstem neuromodulation in the REM-NREM cycle will be introduced in more details later.

Gamma-aminobutyric acid (GABA)

GABA is the main inhibitory neurotransmitter in the central nervous system. GABA-containing neurons involved in sleep-wake regulations mainly locate in the hypothalamic preoptic area, the mesopontine tegmental area and the basal forebrain [25-27]. Cell groups in different locations have distinct discharge profiles. Evidence [25, 26, 28], including the results of lesion, stimulation and neuron recording studies, shows that GABA-containing neurons in preoptic area (POA) are sleep-promoting. They can inhibit the monoaminergic neurons [10, 29-34], particularly the histamine-containing neurons in the posterior hypothalamus. GABA-containing neurons located in the brainstem have been reported to have local interactions between cholinergic neurons in PPT/LDT, serotoninergic neurons in DR and noradrenergic neurons in LC, and take part in the regulation and generation of NREM-REM alternations [33, 35-43]. GABAergic neurons in the basal forebrain are assumed to be sleep-promoting neurons according to their discharge profiles [44]. The controlling mechanisms of different GABA-containing cell groups are also different.

Circadian and Homeostatic Processes

Circadian Process

The circadian signal, which is originated in the suprachiasmatic nucleus (SCN), serves as the brain's master clock [45], the entrainment of which by the daily light-dark cycle sets the 24-hour rhythm for all other physiological rhythms in the organism. Loss of SCN abolishes the circadian rhythms of a range of behavioral and physiological process, including sleep [46]. The link between the SCN and the sleep system has been the subject of much recent investigation [45, 47, 48]. A schematic diagram to illustrate the three-stage integrator for circadian rhythms is shown in Fig. 3. The SCN has relatively modest projections to the VLPO or the orexin neurons in LHA. However, the bulk of its output is directed toward the adjacent subparaventricular zone (SPZ) and the dorsomedial nucleus of the hypothalamus (DMH) [49, 50]. Cell-specific lesions of the ventral SPZ disrupt the circadian rhythms of sleep and wakefulness. Therefore, direct projections from the SCN to sleep are not sufficiently strong to maintain the circadian rhythms in sleep-wake cycle, and the relay neurons in the ventral SPZ are required.

The SPZ also has relatively limited projections to the components of the sleep-wake regulatory system, such as VLPO and orexin in LHA [51-53]. However, a major target of SPZ is the DMH [53, 54], which receives inputs from many more neurons in the SPZ than the SCN. Therefore, the SPZ is in a position to amplify the output of the SCN.

The DMH is one of the largest sources of input to the VLPO and orexin neurons in LHA [52, 55] and crucial for conveying SCN influence to the sleep-wake regulatory system [56]. Cell-specific lesions of the DMH also profoundly diminish circadian rhythms of sleep and wakefulness.[57]. The projection of DMH to the VLPO comes largely from GABA-containing neurons and the projection to the LHA originates from neurons containing glutamate and thyrotropin-releasing [57]. Therefore, I consider the projection from DMH to LHA as activation and projection to VLPO as inhibition.

Additionally, the DMH has relatively few direct outputs to the brainstem components of the ascending arousal system, but the orexin neurons have extensive projections to these targets.

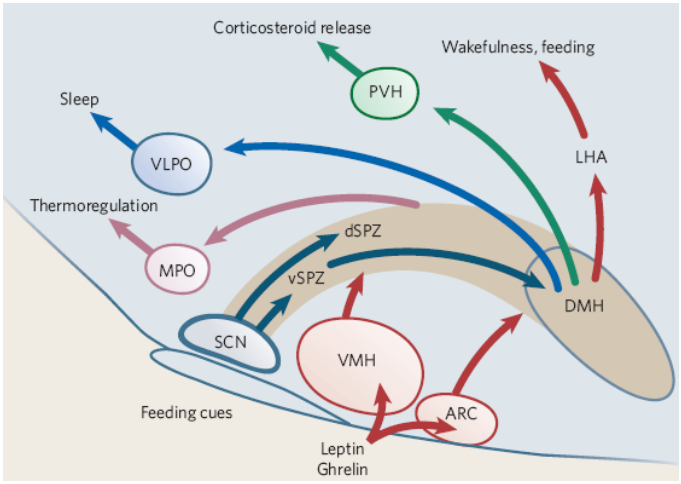

Fig. 3. Schematic diagram illustrating the three-stage integrator for circadian rhythms. Please see [45] for abbreviations not mentioned above.

Homeostatic Process

Although the purpose of sleep remains unknown, it clearly has a restorative effect on the brain. Like other homeostatic systems, sleep deprivation is followed by extra recovery sleep that is proportional to the sleep loss. An influential model of sleep regulation, proposed by Borbely [58], includes both effects of homeostatic and circadian processes for sleep analysis. The homeostatic influence is believed to be due to some structure or substance that accumulates need to sleep during wakefulness, and dissipates this homeostatic need during sleep. Although the mechanism for the homeostatic determinant remains unclear, NREM and REM sleep may probably have separate homeostatic mechanisms.

Some endogenous substances, such as adenosine, cytokines and prostaglandin D_2, have been proposed as homeostatic accumulators of the need of sleep [59-65]. Recent study shows that during prolonged wakefulness, extracellular adenosine levels rise in some parts of the brain, including the basal forebrain [66, 67]. Injection of adenosine or

an adenosine A1 receptor agonist into the basal forebrain of cats [68], or an adenosine A2a receptor agonist near the VLPO in rats [69], directly causes sleep. Hence, one possible mechanism for homeostatic sleep drive might be an accumulation of a sleep-promoting substance that enhances the activity of sleep-promoting cells and reduces the activity of wake-promoting neurons.

Models of Sleep-Wake Cycle

More than 70 years ago, von Economo predicted a wake-promoting area in the posterior hypothalamus and a sleep-promoting region in the preoptic area. In subsequent years, his observations were reproduced by lesion experiments in the brains of animals. More and more neurobiological and physiological findings and recent advances in molecular, cellular and subcortical networks have improved our understanding and view of brain circuitry that regulates our daily cycles of sleep and wakefulness into a new level.

Two processes [58, 70], the circadian and the homeostatic process, are proposed to control and determine the timing and structure of sleep. Under these two processes, the neuron network, including cell groups in the brainstem, hypothalamus, preoptic area and basal forebrain, has been investigated in many studies [1, 5, 45, 71, 72].

The ascending arousal system, firstly proposed by von Economo, is believed to be in charge of the activation of thalamus and cortex, maintaining the wakefulness. This ascending arousal system originates in the brainstem and has two major branches for its upstream pathway. The first branch, originating in the acetylcholine-producing cell groups in PPT/LDT, projects directly to the thalamus and the cerebral cortex. The second branch, originating in the monoaminergic neurons in the brainstem (including the noradrenergic neurons in LC, serotoninergic neurons in DR and histaminergic neurons in TMN), passes lateral hypothalamic area and basal forebrain, through which it eventually

activates the cerebral cortex. The input to the cerebral cortex is augmented by lateral hypothalamic peptidergic neurons (containing melanin-concentrating hormone or orexin).

Most of the cell groups in the ascending arousal system are wake-promoting components and inhibited during sleep by a sleep-promoting system of GABA-containing neurons in preoptic area. Mutual inhibition (Figs. 4a and b) between the arousal- and sleep-producing circuitry results in switching properties that define discrete wake and sleep states, with sharp transitions between them. A flip-flop model [45, 71], shown in Fig. 4c, has been proposed as switch to describe the reciprocal relationship between GABA-containing cell groups in the preoptic area and the major monoamine groups. When GABA-containing VLPO (or eVLPO) neurons fire rapidly during sleep, they are thought to inhibit the monoaminergic cell groups, thus disinhibiting and reinforcing their own firing. Similarly, when monoamine neurons fire at a high rate during wakefulness, they would inhibit those sleep-promoting neurons, thereby disinhibiting their own firing. These two halves of a flip-flop circuit, by each strongly inhibiting the other, create a feedback loop that is bistable, with two possible stable patterns of firing and a tendency to avoid intermediate states.

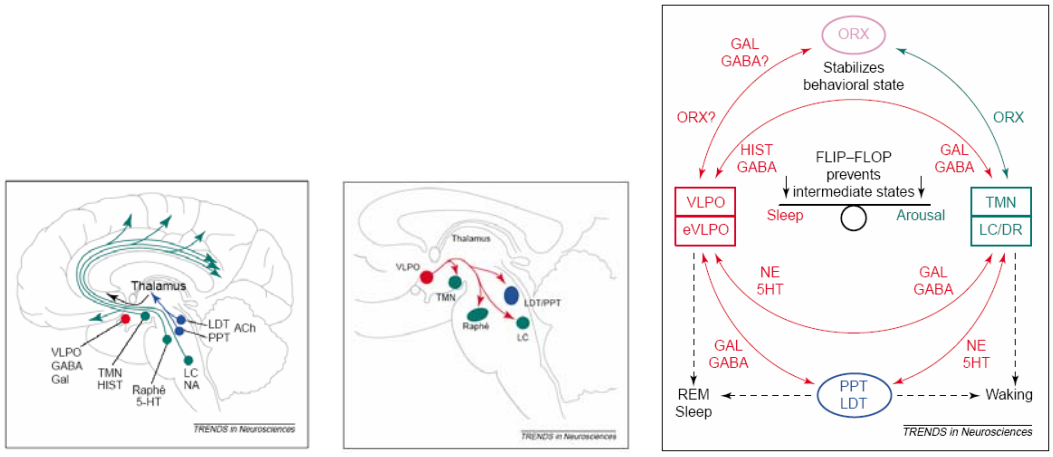

a b c

Fig. 4. Flip-flop model of reciprocal interactions between sleep- and wake-promoting brain regions. (a) The ascending arousal system sends projections from the brainstem and posterior hypothalamus throughout the forebrain. (b) Projections from the VLPO to the main components of the ascending arousal system. (c) Model structure. Please see [71] for details.

Another interesting aspect of the sleep-wake cycle that has received much attention is the generation and regulation of REM (rapid-eye-movement) sleep [11, 63, 72-75]. The original reciprocal-interaction model [76, 77] of NREM-REM alternation proposed that aminergic REM-OFF and cholinergic REM-ON neurons of the mesopontine junction reciprocally interact in a manner that results in the ultradian alternation of mammalian REM and NREM sleep. During waking, the aminergic system is tonically activated and inhibits the cholinergic system. During NREM sleep, aminergic inhibition wanes and cholinergic excitation waxes. At REM sleep onset, aminergic inhibition is shut off, and cholinergic excitability peaks (Fig. 5a). A further study [74] has provided evidence that intermediary non-cholinergic neurons might exist for mediating the interactions between REM-ON and REM-OFF cell groups. A revised mesopontine regulator [72, 74] of NREM-REM alternation is shown in Fig. 5b. Although other studies may have argued for different hypotheses for NREM-REM alternation (for instance, a putative flip-flop switch for REM sleep control was proposed by Saper [75]), the basic idea of interactions between identified REM-OFF and REM-ON neurons is the same. Therefore, I will follow the basic structure of Figs. 5b in this work.

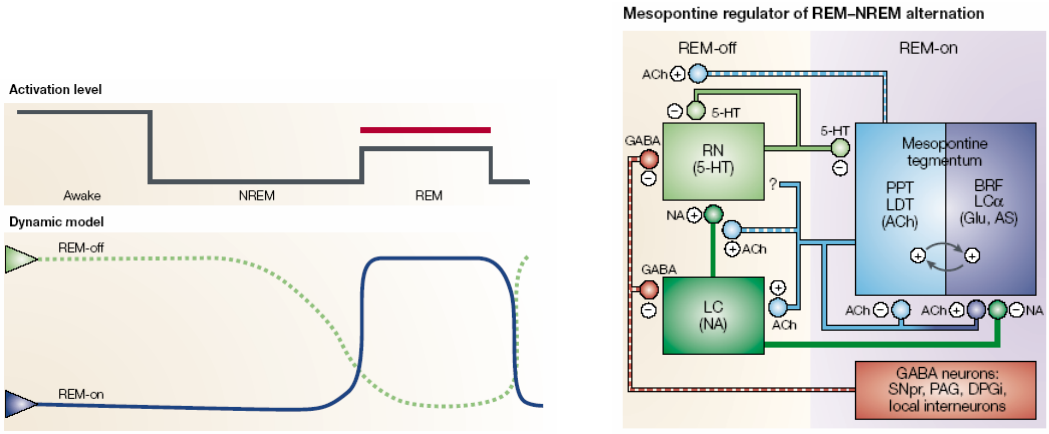

a b

Fig. 5. Reciprocal-interaction model of NREM-REM alternation. (a) Activation model showing the alternation of REM (red bar) and NREM sleep states, and the underlying dynamic model of alternating activity of REM-OFF and REM-ON in pontine nuclei. (b) Mesopontine regulator of REM-NREM alternation. Main abbreviations: BRF, brainstem reticular formation; SNpr, substantia nigra pars reticularis; PAG, periaqueductal grey area. Please see [72] for details.

Except for these biological models of the sleep-wake cycle, there are also a few mathematical models [58, 70, 78-81] describing how the sleep-wake cycle is regulated. Most of these models either do not comprehensively include the function of the neuron groups or do not include all relevant neurons groups. The recent work of Nakao et al. [81] has proposed a mathematical model of the mechanisms orchestrating a quartet neural system of sleep and wakefulness, and this model describes the relationship and controlling mechanism between the upper sleep and wake states and lower neuron network quite well. Compared with their work, I will use a different, more generic modeling method for the sleep-wake cycle.

CHAPTER 2

MODELING METHOD

In this chapter, I briefly introduce the S-system modeling method and apply it to the sleep-wake cycle.

Introduction to the S-system Method

S-systems [82, 83] are at the core of a modeling method that can be applied to analyze and simulate biochemical and biological systems. It is derived from a general system description through well-founded mathematical methods of approximation theory. Compared with traditional biochemical modeling methods, the S-system has the advantage of analytical convenience. It has the following general form of system ordinary differential equations:

$$\dot{X}_i = \alpha_i \prod_{j=1}^{n+m} X_j^{g_{ij}} - \beta_i \prod_{j=1}^{n+m} X_j^{h_{ij}} \quad for \quad i = 1, 2, \ldots, n. \qquad (1)$$

The left-hand side of the equation indicates the time derivative of each dependent variable X_i (changing rate). The right-hand side consists of two parts. The first term is the production term (also called $\alpha - term$), representing the production of X_i or any material flowing into the pool X_i; the second term is the degradation term (also called $\beta - term$), representing the degradation of X_i or any material flowing out of the pool X_i. The system has n dependent variables and m independent variables (whose dynamics is not determined by the system). The parameters α_i, β_i are both constant non-negative factors, representing the rate constants of production and degradation, respectively. The parameters g_{ij}, h_{ij} are also constant values, representing the kinetic orders for chemical reactions or the intensity of interactive actions for others. Usually,

active action corresponds to positive values of g_{ij} *and* h_{ij}, inhibitory action gives negative values of g_{ij} *and* h_{ij}, and no action makes zero values of g_{ij} *and* h_{ij}.

For a typical biochemical system, it has been shown many times that the S-system method can be applied and has a number of advantages. Here I intend to use the method to model the sleep-wake cycle system, and this requires first that I explore the applicability of S-systems for the sleep-wake cycle system, a physiological system involved with neural interactions. I thus begin by testing basic neuronal actions with S-system methods.

Basic Neural Action Testing with S-system Method

In real neurons, the resting membrane potential (usually around -60 mV) is the point at which sodium influx is exactly balanced by potassium efflux. When a chemical substance (called neurotransmitter) is released at the synapse due to the presynaptic action potential, a postsynaptic action potential will be generated in the following. This basic long-distance signal is a self-propagating depolarization; it arises through a sequence of voltage-dependent changes in the ionic permeability of the neuron membrane and an all-or-nothing event. At the end of an action potential, the membrane potential becomes transiently more negative than the threshold (resting potential), which means the cell is hyperpolarized. Therefore, there are three distinctive membrane potentials of a single neuron cell: depolarized, hyperpolarized and resting potential.

However, when we categorize neurons in “ON” and “OFF” states, only the cells with depolarized membrane potential (action potential) can be considered as in “ON” state. Neurons with two other kinds of membrane potentials are thought as in “OFF” state. Furthermore, in this work I will pay more attention to the firing activity of groups of neurons instead of a single cell. In this way, two states “OFF/ON” could better describe the average/overall firing intensity of that neuron group than the three distinct membrane potentials.

Similar to the excitatory and inhibitory synapses that may exist between neurons, we add activating or inhibitory actions between the corresponding neuron groups. Here, we test four basic actions between neurons with S-systems: (1) inhibition; (2) activation; (3) self-inhibition; (4) self-activation. Although inhibitory and excitatory projections might co-exist between neuron groups, only the main projection is taken into account here.

Inhibition and Activation Testing with S-system Method

Let us consider a small neuronal system consisting of two dependent variables and two independent variables (inputs). Each variable receives activation from one input and inhibition from the other input. By using the S-system method, the system can be mathematically formulated as the following:

$$\begin{aligned} \dot{X}_1 &= \alpha_1 S_1^{g_{11}} S_2^{g_{12}} - \beta_1 X_1^{h_{11}} \\ \dot{X}_2 &= \alpha_2 S_1^{g_{21}} S_2^{g_{22}} - \beta_2 X_2^{h_{22}} \end{aligned} \qquad (2)$$

where S_1, S_2 indicate the inputs and we assume that the degradation of X_i only depends on itself, that is $h_{ij} = 0, if\ i \neq j$. Given appropriate parameter values of α, β, g, h and the input signals, we can easily perform simulations with the system equations (2). When input S_1 has high intensity and input S_2 has low intensity, X_2 is activated to the "depolarized" level and X_1 is inhibited to the "hyperpolarized" level; When S_1 and S_2 are all of low intensity, both X_1 and X_2 automatically return to their "resting potential" levels; While S_2 has high intensity and S_1 has low intensity, X_1 is activated to the "depolarized" level and X_2 goes to the "hyperpolarized" level. From the result shown in Fig. 6b, we can see that with appropriate input signal and parameter values, we can simulate different levels of firing activity for a neuron group and cause the neuron group to switch between ON and OFF states by simply changing the input signals.

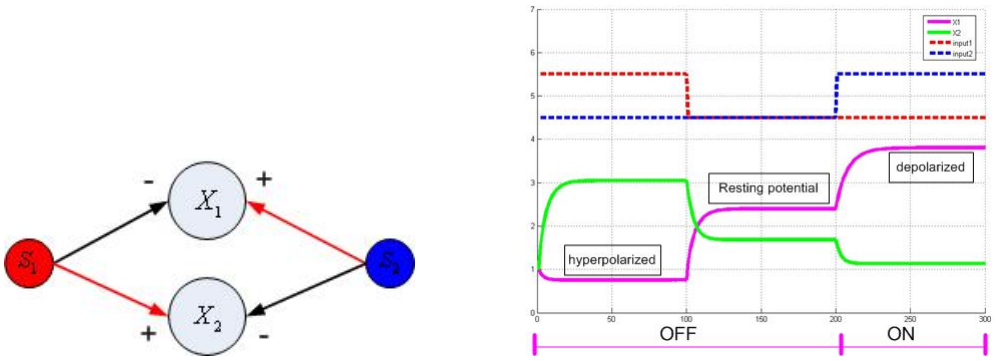

a b

Fig. 6. Inhibition and activation test with S-system method. (a) System structure; (b) Preliminary simulation result. For concrete parameter values and implementation details, please see APPENDIX 1.

Self-Action in S-systems

For some kinds of neurons, their releasing neurotransmitters may affect (inhibit /activate) their own receptors. Furthermore, within a neuron group, some neurons may trigger other neurons in the same group to be activated or inhibited. I use the self-inhibition/self-activation of neurons to simulate these types of phenomena.

For a system containing self-action, firstly let us consider the simplest case shown in the upper part of Fig. 7. By using the S-system method, both cases of self-activation and self-inhibition can be formulated by the following mathematical equation:

$$\dot{X}_1 = \alpha_1 S_1^{g_{1s}} X_1^{g_{11}} - \beta_1 X_1^{h_{11}} \qquad (3)$$

When $g_{11} > 0$, the variable X_1 has self-activation; when $g_{11} < 0$, the variable X_1 exhibits self-inhibition. With a set of appropriate parameter values and the correct input signal, we can obtain the simulation result shown in the lower part of Fig. 7. When X_1 has self-activation, as shown in Fig. 7a, it will have higher intensity of firing activity and longer duration of staying in the ON state compared with the normal case without self-activation. For a neuron with self-inhibition, the opposite result occurs (Fig. 7b), the neuron with self-inhibition will have lower firing intensity and shorter duration of staying in the ON state even with the same input signal.

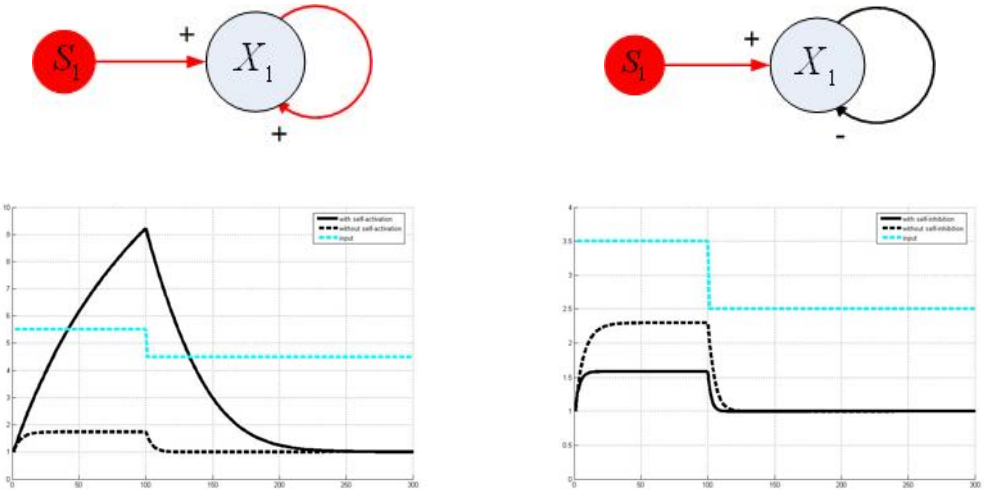

a b

Fig 7. Self-action test with S-system method. (a) Self-activation case; (b) Self-inhibition case. The dashed black lines indicate the normal case without self-action. The blue dashed lines indicate the input. For concrete parameter values and implementation details, please see APPENDIX 1.

In conclusion, the generic tests of activation, inhibition, self-activation and self-inhibition of neurons indicate that the S-system method is rich enough for modeling the principles of the sleep-wake cycle. The biological meaning of the parameters g can be directly interpreted as the projections between or within different neuron groups. As a consequence, corresponding constraints of g can be applied to the system equations. The biological meanings of the parameters h, α *and* β are not as intuitive, and thereby allow some flexibility in implementation.

CHAPTER 3

TWO-PHASE MODEL OF THE SLEEP-WAKE CYCLE

In this chapter, we develop a two-phase model of the sleep-wake cycle. First, the model is treated as an open-loop system, and then the homeostatic regulator is introduced, making the system work as a closed-loop system. The biological considerations, model structure, mathematical description and implementations of the model will be introduced separately in detail.

Biological Considerations

Many research studies show that different neuron groups may have different discharge profiles. During wakefulness, wake-promoting neurons (neurons in LC, DR, LHA, and TMN) [84-89] usually have the highest firing rates and inhibit sleep-promoting neurons (neurons in VLPO and eVLPO) to cause them almost to cease firing. When sleep is occurring, the firing activity of wake-promoting neurons decreases, and the sleep-promoting neurons begin to increase their activity. As sleep continues, some wake-promoting neurons cease firing (or have a low firing rate); some wake-promoting neurons have a slower firing rate during NREM sleep and almost stop firing in REM sleep. These types of neurons are usually called “REM-OFF” neurons. Additionally, there is a special kind of neuron [24] located in PPT/LDT, discharging much higher during REM sleep than NREM sleep and wakefulness. Neurons with this kind of discharge pattern are called “REM-ON” neurons. The discharge profiles of different neuron groups during three distinct behavioral states are listed in Table 1.

Although some experimental results show that several subsets might exist within the same neuron group, the results also indicate that some neuron group may not have a uniform discharge profile: at the very beginning, only the main discharge pattern of each

neuron group is taken into account. We will consider and incorporate other subsets that may have different regulatory roles in later steps.

Table 1. Discharge profiles of different neuron groups during three distinct behavioral states. Firing rates are as follows: ↑↑ = rapid firing; ↑ = slower firing; 0 = little or no firing; Question mark represents hypothesized firing pattern for which there is no firm evidence yet.

	Wakefulness	NREM	REM
LC(NA)	↑↑	↑	0
DR(5-HT)	↑↑	↑	0
TMN(HIS)	↑↑	↑	0
LHA(ORXIN)	↑↑	0?	↑?
PPT/LDT(ACH)	↑	0	↑↑
VLPO(GABA,GAL)	0	↑↑	↑?
eVLPO(GABA,GAL)	0	↑?	↑↑

Open-Loop Two-Phase Model

Model Structure

According to the known discharge profiles of neuron groups and the possible biological mechanisms of the sleep-wake cycle introduced in Chapter 1, I developed a two phase model of the sleep-wake cycle. The first phase addresses the switch between wakefulness and sleep, which is controlled by the reciprocal inhibition between some wake-promoting and sleep-promoting neurons. This switch is in phase with the rhythm of external circadian signals. When the circadian signal is strong (during daytime), it will activate wake-promoting neurons and inhibit sleep-promoting neurons, making the behavioral state stay in WAKE. As night approaches, the circadian signal becomes weak,

inducing the decreasing firing activity of wake-promoting neurons. Thus, it is the turn of sleep-promoting neurons to increase their activity, and the behavioral state switches from WAKE state to the SLEEP state. The second phase is related to NREM-REM alternation, which is believed to be under the regulation of REM-OFF and REM-ON neurons in the mesopontine. Once sleep occurs, the behavioral state first comes into NREM state and "REM-OFF" neurons still have relative low firing rate. As sleep continues, the further inhibition from the sleep-promoting neurons causes the firing activity of REM-OFF neurons to become weaker and weaker, which releases REM-ON neurons from the inhibition of REM-OFF neurons and the behavioral state enters REM state. In REM sleep, REM-ON neurons can activate themselves and also REM-OFF neurons, which will finally turn on REM-OFF neurons and make the behavioral state alternate between NREM and REM. In other words, the sleep-wake cycle system experiences two rhythms, one goes with the external circadian signal, the other is generated by the system itself. The switches of behavioral states between WAKE, NREM and REM are under the regulation of underlying REM-ON, REM-OFF, sleep-promoting and wake-promoting neurons through their interactions. The structure of the open-loop two-phase model is shown in Fig. 8.

Further investigation shows that neurons in VLPO and eVLPO have a similar discharge profile, although they may have different efferents/afferents or possible regulating roles [26, 28]. Similarly, neurons in LC and DR, neurons in BRF and PPT/LDT also have similar discharge patterns and possible regulating roles although they locate in different areas and have different neurotransmitters [13, 35, 38, 43, 85, 87, 89-91]. Based on these observations, one could introduce some reasonable system simplifications as following: (1) treat VLPO and eVLPO as one sleep-promoting variable in order to avoid some uncertain interactions for clearly separating VLPO and eVLPO; (2) combine LC and DR as one "REM-OFF" variable and treat the actions between them as self-actions; (3) combine BRF and PPT/LDT as one "REM-ON" variable and consider the actions

between them as self-actions. With these simplifications, we obtain a simplified structure of the previous system as shown in Fig. 9a. The NREM-REM alternation can correspondingly be expressed by a two-dimensional REM-OFF and REM-ON oscillating system shown in Fig. 9b, which is more convenient and easier with respect to implementation.

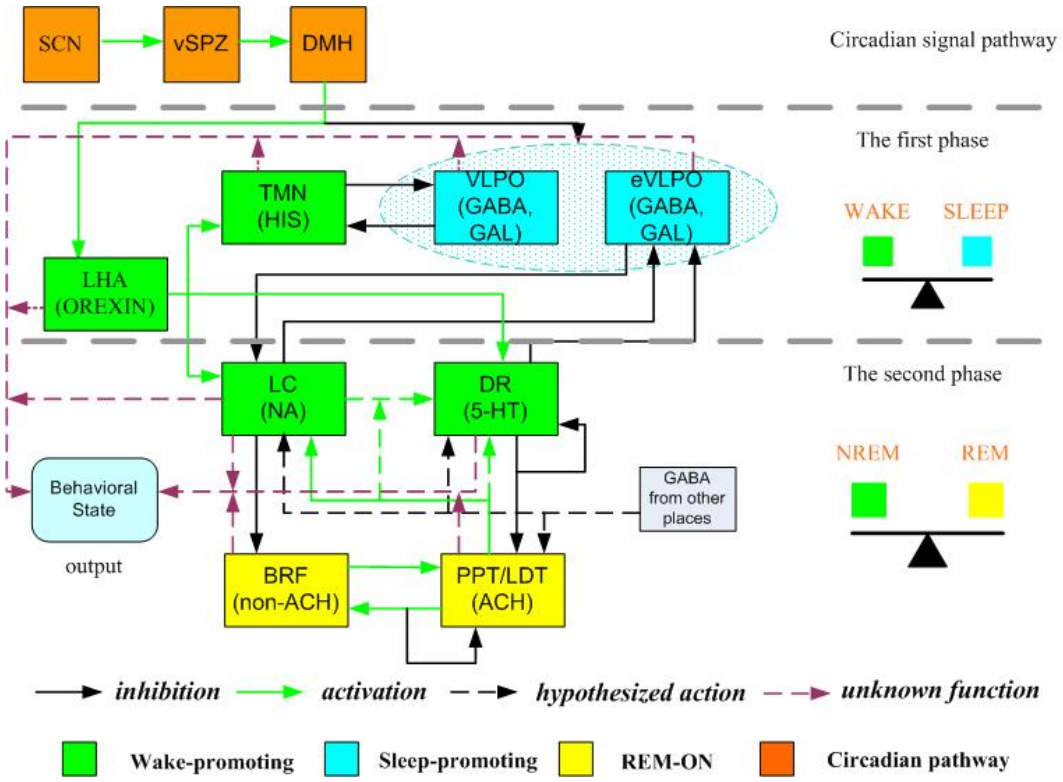

Fig8. Structure diagram of the open-loop two-phase model. The two gray dashed lines separate the whole structure into three parts. The upper part is about the circadian signal pathway; the middle part is the first phase; the lower part is the second phase. Different colors of the boxes represent the possible regulating roles. Neurotransmitter (if have) and location of each neuron group are listed in the box.

Mathematical Description

I now use the S-system method to model the sleep-wake cycle. Each dependent variable in the system X_i indicates the average/overall firing activity of one neuron group, which can be intuitively interpreted as the percentage of activated neurons among

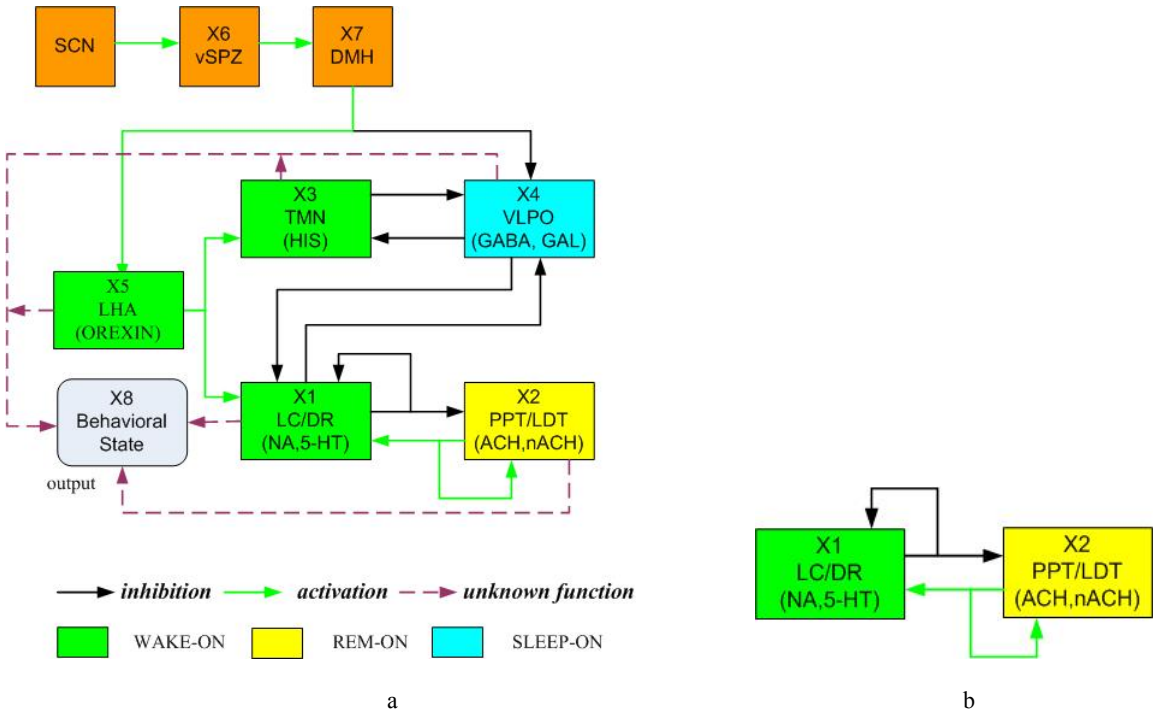

Fig. 9: Structure diagram of the simplified open-loop two-phase model. (a) Structure of the entire system. (b) Structure of 2D REM-OFF and REM-ON oscillating system. Different colors of the boxes represent the possible regulatory roles. Neurotransmitters (if existent) and location of each neuron group are listed in the box.

the whole group. The maximum value of X_i indicates that a group of neurons has been completely turned on. The only independent variable is the external circadian signal, which has 24-hour periodicity. Moreover, according to the biological meanings of g_{ij}, some constraints can be automatically added to the mathematical system equations; for instance, no projections between variables X_i and X_j indicate the parameter g_{ij} should be zero. According to the model structure shown in Fig. 9, by using the S-system method, the simplified open-loop two-phase model can be formulated as following:

$$
\begin{aligned}
\dot{X}_1 &= \alpha_1 X_1^{g_{11}} X_2^{g_{12}} X_4^{g_{14}} X_5^{g_{15}} - \beta_1 X_1^{h_{11}} \\
\dot{X}_2 &= \alpha_2 X_1^{g_{21}} X_2^{g_{22}} - \beta_2 X_2^{h_{22}} \\
\dot{X}_3 &= \alpha_3 X_4^{g_{34}} X_5^{g_{35}} - \beta_3 X_3^{h_{33}} \\
\dot{X}_4 &= \alpha_4 X_1^{g_{41}} X_3^{g_{43}} X_7^{g_{47}} - \beta_4 X_4^{h_{44}} \\
\dot{X}_5 &= \alpha_5 X_7^{g_{57}} - \beta_5 X_5^{h_{55}} \\
\dot{X}_6 &= \alpha_6 [SCN]^{g_{6s}} - \beta_6 X_6^{h_{66}} \\
\dot{X}_7 &= \alpha_7 X_6^{g_{76}} - \beta_7 X_7^{h_{77}} \\
X_8 &= output\ \ fun(X_1, X_2, X_3, X_4, X_5)
\end{aligned}
\tag{4}
$$

where $X_1 \cdots X_5$ are dependent variables, respectively representing neuron groups in LC/DR(NA,5-HT), PPT/LDT(ACH, non-ACH), TMN(HIS), VLPO(GABA,GAL), LHA(ORX), vSPZ, DMH; SCN, the only independent variable, represents circadian signal. X_6, X_7 are also dependent variables, representing the pathway through which the circadian signal could regulate the sleep-wake cycle; their main function is to act as an amplifier to increase the intensity of circadian signal. X_8 represents the output behavioral state, which has only three discrete values, respectively representing WAKE, NREM and REM. The value of X_8 is determined by the firing activities of all neuron groups.

Totally, 36 parameters (22 for g_{ij} and h_{ij}, 14 for α_i, β_i) in this system need to be pursued. Among these parameters, some have constraints due to the biological interactions. The parameter constraints can be expressed as follows:

(1) $g_{11} < 0, g_{12} > 0, g_{14} < 0, g_{15} > 0$; (2) $g_{21} < 0, g_{22} > 0$; (3) $g_{34} < 0, g_{35} > 0$; (4) $g_{41} < 0, g_{43} < 0, g_{47} < 0$; (5) $g_{57} > 0$; (6) $g_{6s} > 0$; (7) $g_{76} > 0$; (8) $\alpha_i > 0, \beta_i > 0\ (i = 1 \cdots 7)$.

For the system of ordinary different equations (4) and corresponding parameter constraints, in order to achieve a good simulation result, it is necessary to find a set of reasonable parameter values that not only satisfy those constraints, but also make the

solutions of the ordinary differential equations consistent with the biological observations and our assumptions. Considering the second phase of the model has a nearly sustained oscillation, we investigate the parameters involved in the 2D oscillating system shown in Fig. 9b and customize a limit cycle for NREM-REM alternations for the first implementation step.

2D Limit Cycle

A limit cycle [92] on a two-dimensional manifold is a closed trajectory in phase plane having the property that at least one other trajectory spirals into it either as time approaches infinity or as time approaches minus infinity. In the case where all the neighboring trajectories approach the limit cycle as time goes to infinity, it is called a stable or attractive limit cycle. Stable limit cycles imply self-sustained oscillations; any small perturbation from the closed trajectory causes the system to return to the limit cycle. For two-dimensional nonlinear systems, different criteria exist for generating a stable limit cycle, such as the criterion based on Hopf bifurcations and the Kolmogorov criterion [93] for models like prey-predator systems. Since our system has a special mathematical format, we prefer the Hopf bifurcation method to customize a stable limit cycle.

Hopf Bifurcation

Subject to certain restrictions, the Hopf bifurcation theorem predicts the appearance of a limit cycle about any steady state that undergoes a transition from a stable to an unstable focus as some parameter is varied. The result is local in the following sense: (1) the theorem only holds for parameter values close to the bifurcation value. (2) The predicted limit cycle is close to the steady state. A key requirement is that the given steady state be associated with a pair of complex eigenvalues whose real parts

change sign; in more popular phrasing, such eigenvalues are said to "cross the real axis".

For the special case *n*=2, I consider a system of two equations that contain a parameter γ:

$$\begin{aligned} \frac{dx}{dt} &= f(x, y; \gamma), \\ \frac{dy}{dt} &= g(x, y; \gamma). \end{aligned} \qquad (5)$$

Here *f* and *g* are assumed to be continuous and differentiable functions. Suppose that for each value of γ the equations admit a steady state whose value may depend on γ, that is $(\overline{x}(\gamma), \overline{y}(\gamma))$. Consider the Jacobian matrix evaluated at the parameter-dependent steady state:

$$J(\gamma) = \begin{pmatrix} \frac{\partial f}{\partial x} & \frac{\partial f}{\partial y} \\ \frac{\partial g}{\partial x} & \frac{\partial g}{\partial y} \end{pmatrix}_{(\overline{x}, \overline{y})} \qquad (6)$$

Suppose the eigenvalues of this matrix are $\lambda(\gamma) = a(\gamma) \pm b(\gamma)i$, and there is a value γ^*, called the bifurcation value, such that $a(\gamma^*) = 0, b(\gamma^*) \neq 0, and\ da/d\gamma \neq 0\ at\ \gamma = \gamma^*$, which means that as γ is varied through γ^*, the real part of the eigenvalues change sign.

Given these hypothesis, the following possibilities arise:

1. At the value $\gamma = \gamma^*$ a center is created at the steady state, and thus infinitely many neutrally stable concentric closed orbits surround the point $(\overline{x}, \overline{y})$.
2. There is a range of γ values such that $\gamma^* < \gamma < c$ for which a single closed orbit (a limit cycle) surrounds $(\overline{x}, \overline{y})$. As γ is varied, the diameter of the limit cycle changes in proportion to $\left|\gamma - \gamma^*\right|^{1/2}$. There are no other closed orbits near $(\overline{x}, \overline{y})$. Since the limit cycle exists for γ values above γ^*, this phenomenon is known as a supercritical bifurcation.

3. There is a range of values such that $d < \gamma < \gamma^*$ for which a conclusion similar to case 2 holds. The limit cycle exists for γ values below γ^*, and this is termed a subcritical bifurcation.

Furthermore, to determine whether or not the limit cycle is stable, a rather complicated calculation must be performed. A simple case is given by the following. For the system of equations (5), it is assumed that for $\gamma = \gamma^*$ the Jacobian matrix is of the form:

$$J = \begin{pmatrix} 0 & 1 \\ -b & 0 \end{pmatrix} \qquad (7)$$

In this case the eigenvalues at $\gamma = \gamma^*$ are $\lambda_{1,2} = \pm bi$, then the following expression must be calculated and evaluated at the steady state when $\gamma = \gamma^*$:

$$V''' = \frac{3\pi}{4b}(f_{xxx} + f_{xyy} + g_{xxy} + g_{yyy}) + \frac{3\pi}{4b^2}[f_{xy}(f_{xx} + f_{yy}) + g_{xy}(g_{xx} + g_{yy}) + f_{xx}g_{xx} - f_{yy}g_{yy}] \quad (8)$$

Then the conclusions are as follows:

1. if $V''' < 0$, then the limit cycle occurs for $\gamma > \gamma^*$ (supercritical) and is stable.
2. if $V''' > 0$, then the limit cycle occurs for $\gamma < \gamma^*$ (subcritical) and is unstable.
3. if $V''' = 0$, the test is inconclusive.

If the Jacobian matrix obtained by linearization of equations (5) has diagonal terms but the eigenvalues are still complex and on the imaginary axis when $\gamma = \gamma^*$, then it is necessary to transform variables so that the Jacobian appears as in (7), before the stability recipe can be applied.

A Criterion for Hopf Bifurcations in S-systems

To apply the Hopf bifurcation theorem to equations having the mathematical format of an S-system, after the coordinate transformation, a specific criterion for limit

cycles for S-systems has been developed by Lewis [94]. Since the system must have an equilibrium if it is to have a Hopf bifurcation, we may assume, without loss of generality, that the μ - parameterized S-system is written in the form

$$\frac{dx}{dt} = \gamma(x^G - x^H) \qquad (9)$$

where γ, G, H may depend (smoothly) upon μ , and $\gamma \geq 0$. For convenience, we define $Q = G - H$. For the simplest case *n* = 2, the conditions of generating a stable limit cycle can be stated as the following five conditions:

1. $trace([\gamma]Q) = 0$; (*trace*)

2. $\det([\gamma]Q) > 0$; (det)

3. $\frac{d}{d\mu}(trace([\gamma]Q)|_{\mu=\mu_0} \neq 0$ (*changing sign*)

4. Let

$$P = G + H - 2I$$

$$a = \frac{-\gamma_1\gamma_2 q_{12}q_{22}}{64}((\gamma_1 q_{21} + \gamma_2 q_{12})\det(Q) + \gamma_2 q_{21}(p_{12} - p_{22})^2 + \gamma_1 q_{12}(p_{11} - p_{21})^2$$

If $a < 0$ then there is a family of stable limit cycles. If $a > 0$ then there is a family of unstable limit cycles. (*stability sign*)

5. Let $b = \frac{d}{d\mu}(trace([\gamma]Q))|_{\mu=\mu_0}$

If $b > 0$ then the stable limit cycles occur for $\mu > \mu_0$ and the unstable limit cycles occur for $\mu < \mu_0$. If $b < 0$, then the stable limit cycles occur for $\mu < \mu_0$, and the unstable limit cycles occur for $\mu > \mu_0$. (*existing area sign*)

If we assume γ in the form $[1+\mu;\quad 1]$ for the 2-dimenstion S-system, the above conditions can be directly expressed by the parameters of G and H and require parameters in G and H to satisfy the following conditions:

$$(1+\mu_0)(g_{11}-h_{11})+(g_{22}-h_{22})=0 \qquad (trace)$$

$$(1+\mu_0)(g_{11}-h_{11})(g_{22}-h_{22})+(1+\mu_0)(g_{21}-h_{21})(h_{12}-g_{12})>0 \qquad (\det)$$

$$\frac{d}{d\mu}(trace([\gamma]Q))|_{\mu=\mu_0}=g_{11}-h_{11}\neq 0 \qquad (changing\ sign)$$

$$a=\frac{-(1+\mu_0)q_{12}q_{22}}{64}(((1+\mu_0)q_{21}+q_{12})\det(Q)+q_{21}(p_{12}-p_{22})^2+(1+\mu_0)q_{12}(p_{11}-p_{21})^2) \quad (stability\ sign)$$

$$b=g_{11}-h_{11} \qquad (existing\ area\ sign)$$

With these conditions, we can search for sets of parameters of G and H to customize a stable limit cycle for 2-dimensional S-systems. Additionally, we can assign some constraints to the parameters, such as positive, negative or zero values. For a 2D system, we have eight parameters for G and H, and for each parameter there are three possible "signs" (-, 0, +), so that there are a total of $3^8=6561$ possible combinations. By testing the above conditions, there are 4317 combinations that do not generate limit cycles and there are 2244 combinations that show the possibility of generating limit cycles (including stable and unstable ones). By simple investigation, we find that the number of zeroes in parameters can be no more than four for any parameter combination leading to limit cycles. This can be easily understood by testing the conditions above. When the number of zeros is more than four (at least five), the "trace" and "det" conditions can not be satisfied simultaneously. Within these possible combinations, we can easily find a set of parameter values that could construct a stable limit cycle.

Customize a Stable Limit Cycle for NREM-REM Alternation

Considering the two-dimensional NREM-REM oscillating system shown in Fig. 9b and the conditions necessary for customizing a stable limit cycle, four constraints of parameters are generated as the following: (1) $g_{11}<0, g_{21}<0$; (2) $g_{12}>0, g_{22}>0$; (3) $h_{12}=h_{21}=0$; (4) $h_{11}, h_{22}\neq 0$. Under these four constraints, we can easily search a set of parameters to make the corresponding two-dimension NREM-REM oscillating system have a stable limit cycle. An example is shown in Fig. 10.

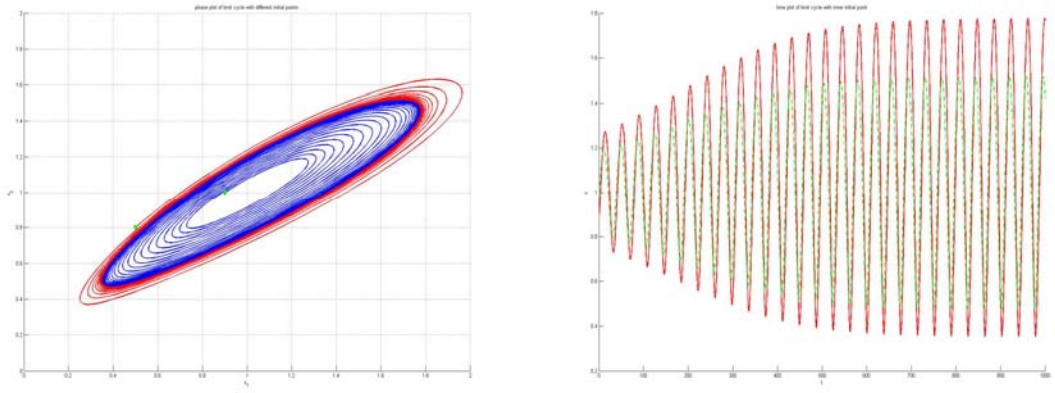

a b

Fig. 10. Limit cycle with right-hand direction. (a) Phase plot of limit cycle with different initial points. (b) Time plot of limit cycle with inner initial point. The green triangles indicate the initial point position. Parameter values are: g = [-0.0338 0.5548; -0.2885 0.7992]; h = [0.33 0; 0 0.4355]; μ = -0.01.

If we look at the time plot of the system (Fig. 10b) carefully, we will find that the peaks of green and red lines always occur simultaneously, which is contrary to the biological observation of discharge pattern of REM-OFF & REM-ON neurons, that is, the peaks of these two kinds of neurons usually occur alternatively. In order to make the simulation result consistent with the observation, we need to change the orientation of the limit cycle shown in the phase plot (Fig.10a) from right to left. By investigation, two more constraints need to be added: (5) $g_{11} > h_{11}$; (6) $g_{22} < h_{22}$. Conditions (1) and (5) together indicate that condition (4) needs to be modified as (4') $h_{11} < 0, h_{22} > 0$. With the newly defined constraints of parameter G and H, we can easily search a set of parameters to customize a left-directed stable limit cycle (Fig. 11a) for the two-dimensional NREM-REM alternation system. As Fig. 11b shows, the peaks of the green line and red line occur alternatively for the left-slanted limit cycle.

Implementation and Discussion

I implemented the simplified open-loop two-phase model of the sleep-wake cycle in MATLAB and obtained some preliminary results. The external circadian signal is

modeled with a stepwise function. The output behavioral state, which should be determined by the firing activities of all neuron groups, is judged actually by the firing activities of OREXIN neurons, REM-OFF neurons and REM-ON neurons for implementation since the activities of other neuron groups give no more information than these three groups. The whole simulation is done for 48 hours (2880 minutes), among which I assume 16 hours for wakefulness and 8 hours for sleep. Given a set of appropriate parameter values, I obtained the simulation results shown in the following figures. The criterion for judging the behavioral state and the concrete values of parameters are given in the APPENDIX 2.

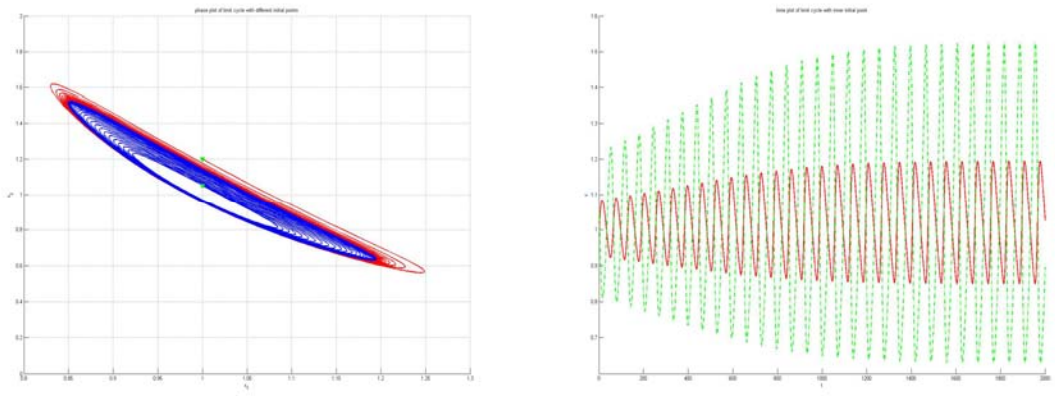

a b

Fig. 11: Limit cycle with left-hand direction. (a) Phase plot of limit cycle with different initial points; (b) Time plot of limit cycle with inner initial point. The green triangles indicate the initial point position. Parameter values are: g = [-0.031 0.211; -1.414 0.2688]; h = [-0.5674 0; 0 0.8053]; $\mu = 0.01$.

Fig12 shows the simulation result of a normal sleep-wake cycle. The relative intensity of external circadian signal indicates different time period of a day. When the intensity of circadian signal is relatively high, the value of behavioral state is 1 (which corresponds to daytime), and wake-promoting neurons (LC&DR, TMN, and OREXIN) have high firing rates, while sleep-promoting neurons (VLPO) and REM-ON neurons exhibit minimal firing activity. When the intensity of the circadian signal becomes weak,

the behavioral state goes away from 1 and sleep period approaches. Neurons in TMN and ORX dramatically decrease their firing rates to the minimal level, and neurons VLPO intensely increase their activity to the maximal level. Meanwhile, REM-OFF (LC&DR) neurons gradually decrease their firing rate and REM-ON (PPT/LDT) neurons begin to increase their activity until the activity of REM-OFF neurons is weak enough. The oscillations between REM-OFF and REM-ON neurons occur and the behavioral state switches between "NREM" and "REM" periodically. Therefore, the discharge activities of all neuron groups and switching pattern of the behavioral state in the simulation result are essentially consistent with the biological observations, indicating the simplified open-loop two-phase model of sleep-wake cycle at least is valid to some degree.

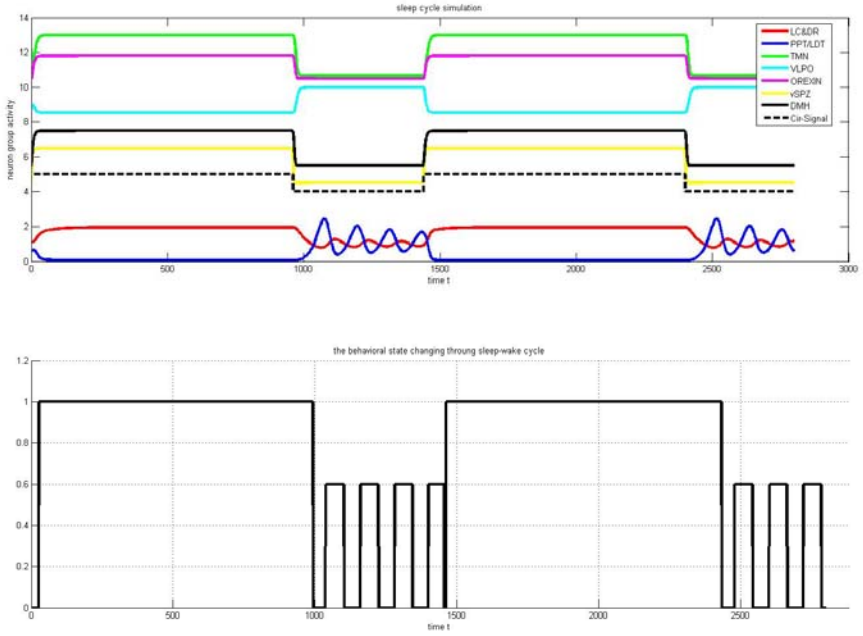

Fig. 12: Simulation results of the open-loop two-phase model for the normal sleep-wake cycle. *Upper Panel:* Firing activity of each neuron group over time. *Lower Panel:* Behavioral state changing over time. The values 0, 0.6 and 1 in the lower plot respectively represent the state NREM, REM, WAKE. Special parameter values: g_{57}= 0.4. Please see APPENDIX 2 for other parameter values.

To further validate the structure of the simplified open-loop two-phase model and identify the role of orexin during the sleep-wake cycle, I implemented two more simulations that allowed for changing the level of orexin. All implementation settings are the same as in the previous simulation except for the parameter explained in the figure legend. The level of orexin can be changed either by modifying the parameter value indicating the efferent projection to orexin or by changing the parameter value indicating the afferent projection from orexin. Both cases have been tested by simulation and they show no differences in results. Here, we only show two results of the former case. In Fig. 13a, the parameter value g_{57} is appropriately enlarged, leading to activity levels of the corresponding wake-promoting neurons that are stronger/higher than normal during wake periods. What's more important is the change in the NREM-REM oscillation. Compared with the normal sleep-wake cycle (Fig. 14a and Fig. 14b), the episodes of REM sleep decrease from four to three and a half, which means the frequency of NREM-REM oscillation is decreased. This simulation result is consistent with the experimental observation [95] that when orexin agonist is injected, the number of REM episodes is reduced. By contrast, Fig. 13b shows that with decreased level of orexin, the activities of wake-promoting neurons are reduced, and the frequency of NREM-REM oscillation is increased a little bit compared to the normal case (Fig. 14a and Fig. 14c), although the increased level is of very small magnitude. These two simulations suggest that orexin is regulating the sleep-wake cycle and that its level is directly affecting the REM sleep. However, the simulation results still have some drawbacks which indicate the limitations of the simplified open-loop two-phase model. First, the duration of each REM episode in the simulation result is almost of the same length due to the limit cycle we customized, while in reality the durations of REM episodes are different from each other and become longer as the sleep becomes increasingly deeper, which indicates that the NREM-REM oscillation is not a pure limit cycle. Secondly, the entire system is totally controlled by the external circadian signal itself, while sleep deprivation and prolonged-wakefulness

experiments have indicated that other factors are also involved in the control system of the sleep-wake cycle. Finally, although the true firing rate of each neuron group may be unknown, the discharge profiles of some neuron groups are probably not as simple as the simulation results show. For example, the firing rate of orexin is not always kept at a minimal level during the entire sleep period. Therefore, we need further modifications of our open-loop two-phase model and incorporate other control signals.

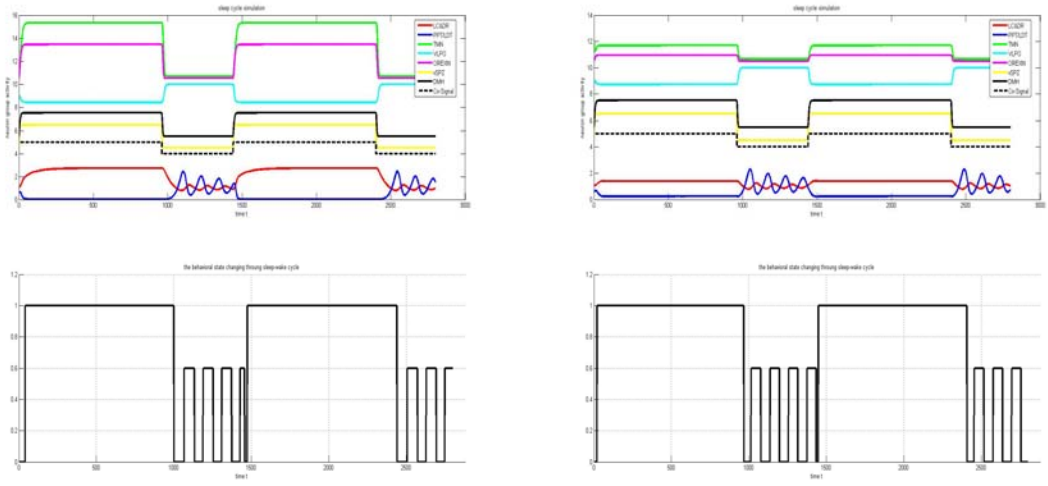

a b

Fig. 13: Simulation results of the open-loop two-phase model for abnormal sleep-wake cycle. (a) With increased level of orexin, special parameter value g_{57}=0.6. (b) With decreased level of orexin, special parameter value g_{57}=0.25. The values 0, 0.6 and 1 in the lower plot respectively represent the behavioral state NREM, REM, WAKE. Please see APPENDIX 2 for other parameter values.

Closed-Loop Two-Phase Model

Biological Considerations

Although the specifics of regulation in the sleep-wake cycle remain unclear, as discussed in Chapter 1, homeostatic processes are involved in the regulation and control of the sleep-wake cycle, along with circadian signals. A representative homeostatic "accumulator" of the need of sleep is extracellular adenosine [67]. Its concentration

varies according to different behavioral states and it is able to activate neurons in basal forebrain via the A_1 receptor [60] and increase the activity of neurons in VLPO via the A_{2a} receptor [69].

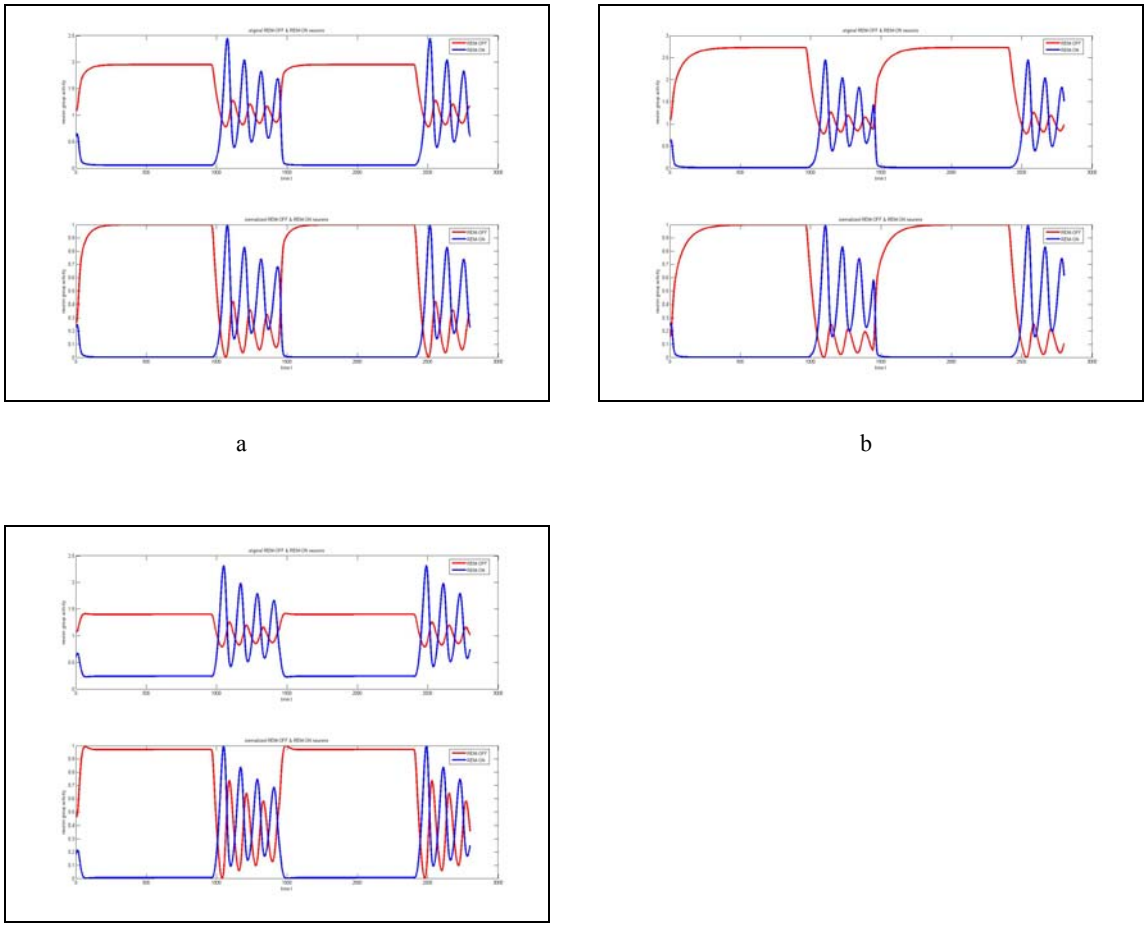

a b

c

Fig14. Simulated firing activities of REM-OFF and REM-ON neurons for different sleep-wake cases. (a) Normal sleep-wake cycle; (b) Abnormal sleep-wake cycle with increased level of orexin; (c) Abnormal sleep-wake cycle with decreased level of orexin. In each sub-figure, the upper plot represents the true va value; the lower plot represents normalized values.

Model Structure

In order to take the role of a homeostatic factor in the regulation of the sleep-wake cycle into account, I incorporated the homeostatic factor into the previous open-loop two-

phase model to construct a closed-loop system, in which the circadian signal and homeostatic factor together control the switches between different behavioral states. The neuron groups taking part in the underlying regulatory network are the same as in the open-loop system: they are neuron groups in LC (NA) & DR (5-HT), PPT/LDT (ACH) & BRF (non-ACH), VLPO & eVLPO (GABA, GAL), TMN (HIS) and LHA (ORX). The input circadian signal still goes through the same pathway to regulate these neuron groups. The output behavioral state is determined by the firing activities of all neuron groups and interacts with the homeostatic regulator, which is assumed to accumulate or dissipate during different states of the cycle. Compared with the open-loop structure of the two-phase model, the newly built-up structure of the closed-loop system has one more dependent variable; it is shown in Fig. 15. To make the implementation simpler, the closed-loop system shown below is following the simplified version of the open-loop system. If one wanted to incorporate more biological details into the system, one could treat the non-simplified version of open-loop system in a similar way and obtain a corresponding closed-loop form of it.

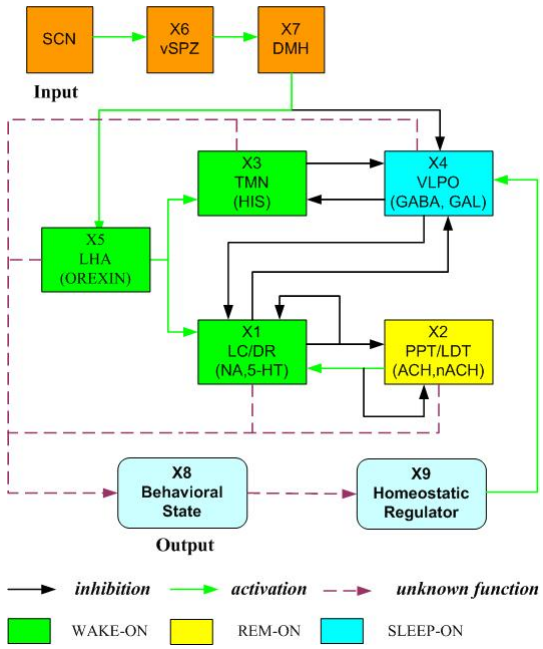

Fig. 15: Structure diagram of the closed-loop two-phase model. Different colors of boxes represent possible regulatory roles. Neurotransmitters (if known) and location of each neuron group are listed in the boxes.

Mathematical Description

According to the model structure shown in Fig. 15, one easily converts the structure diagram into the S-system format as

$$
\begin{aligned}
\dot{X}_1 &= \alpha_1 X_1^{g_{11}} X_2^{g_{12}} X_4^{g_{14}} X_5^{g_{15}} - \beta_1 X_1^{h_{11}} \\
\dot{X}_2 &= \alpha_2 X_1^{g_{21}} X_2^{g_{22}} - \beta_2 X_2^{h_{22}} \\
\dot{X}_3 &= \alpha_3 X_4^{g_{34}} X_5^{g_{35}} - \beta_3 X_3^{h_{33}} \\
\dot{X}_4 &= \alpha_4 X_1^{g_{41}} X_3^{g_{43}} X_7^{g_{47}} [Hom]^{g_{4s}} - \beta_4 X_4^{h_{44}} \\
\dot{X}_5 &= \alpha_5 X_7^{g_{57}} - \beta_5 X_5^{h_{55}} \\
\dot{X}_6 &= \alpha_6 [SCN]^{g_{6s}} - \beta_6 X_6^{h_{66}} \\
\dot{X}_7 &= \alpha_7 X_6^{g_{76}} - \beta_7 X_7^{h_{77}} \\
X_8 &= ouput\ \ fun(X_1, X_2, X_3, X_4, X_5) \\
X_9 \ or\ \dot{X}_9 &= Homeostatic\ \ fun(X_8)
\end{aligned}
\qquad (10)
$$

where $X_1 \cdots X_9$ respectively represent neurons in LC/DR, PPT/LDT, TMN, VLPO, LHA, the circadian pathway vSPZ, DMH, the behavioral state and the homeostatic regulator. Compared with system equation (4), one more equation describing the function of the homeostatic regulator has been added. The homeostatic regulator could positively activate sleep-promoting neurons in VLPO as shown in Fig. 15. Borbely [70] used a recursive formulation (iteration) to describe the homeostatic process, which is increasing during waking and decreasing during sleep. Nakao [81] used linear differential equations to describe two different homeostatic regulators for NREM and REM sleep separately. Although the concrete homeostatic functions are different, the basic idea is the same. That is, homeostatic regulation, whether due to some special structures or to chemical substances, is sleep-promoting. Its intensity is accumulated during wakefulness, and reaches the maximal amount at the end of wakefulness or at the period of sleep deprivation. Once sleep begins, its intensity dissipates and reaches the minimal level at the end of sleep. Considering this common property of the homeostatic regulator, we use the following ordinary differential equation to describe the change of homeostatic regulator:

$$\dot{X}_9 = \delta_{wake}\kappa_w - \delta_{sleep}\kappa_s - \kappa_c X_9 + \eta \qquad (11)$$

where X_9 represents the homeostatic regulator, $\kappa_w, \kappa_s, \kappa_c$ are positive constant parameters, η represents noise, and

$$\delta_{wake} = \begin{cases} 1, & behavioral\ state = WAKE \\ 0, & behavioral\ state = REM\ or\ NREM \end{cases}$$

$$\delta_{sleep} = \begin{cases} 0, & behavioral\ state = WAKE \\ 1, & behavioral\ state = REM\ or\ NREM \end{cases}$$

Implementation and Discussion

I implemented the simplified version of the closed-loop two-phase model in MATLAB and obtained some preliminary results. The simulation extends over 1800 time units, among which I assign roughly 1200 units to wakefulness and 600 units to sleep. The external circadian signal is modeled with one of two functions shown in Fig. 16. The first is a step function, while the other is a smoothed step function. The simulation results with different circadian functions are respectively shown in Fig. 17 and Fig. 18. These figures indicate how decades/increases in the circadian signal affect the subsequent firing activities of different neuron groups, especially the REM-ON neurons, after which the output behavioral state changes. Among the two external functions, the smoothed step function might be preferable because any continuous signal should diminish or decrease gradually. Other neuron variables and circadian signal pathways are modeled in the same way as for the open-loop system before.

Compared with the simulation results of the open-loop system, there are two main differences. One is the activity of neurons in VLPO, which doesn't maintain a constant value as it does in the open-loop system. Since there is reciprocal inhibition between neurons in VLPO and LC/DR, the oscillations of REM-OFF (LC/DR) and REM-ON neurons affect the activity of VLPO and cause it to oscillate slightly. The same is true for neurons in TMN. Moreover, due to the effect of the homeostatic regulator, we can see a

gradually decreasing tendency of the activity of VLPO neurons during sleep. Another difference is evident in the episodes of REM sleep, which are not exactly the same as in the open-loop system.

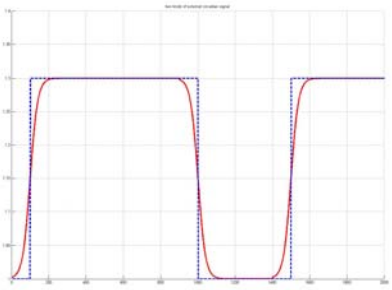

Fig16. Circadian signal functions. The blue dashed line represents the stepwise function; the red line represents the smoothed step function. Please see APPENDIX 3 for specific implementations of the circadian functions.

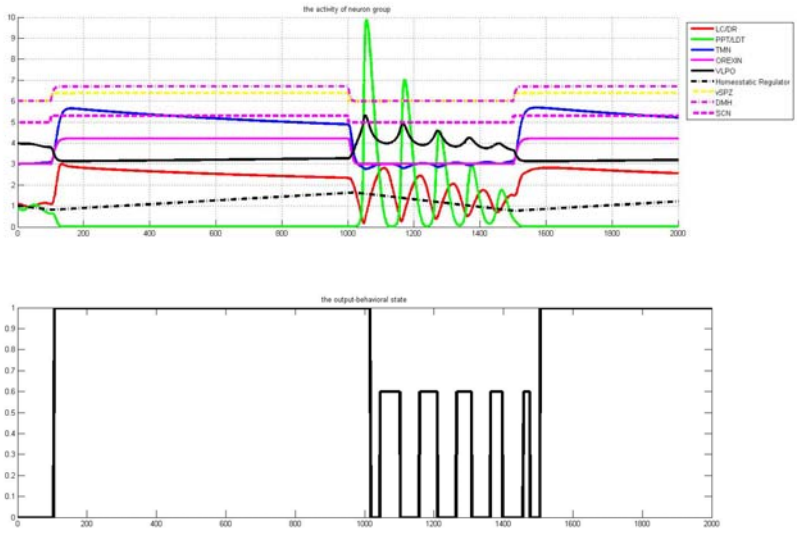

Fig. 17: Simulation result of the closed-loop two-phase model for normal sleep-wake cycle with step circadian function. *Upper Panel*: Firing activity of each variable. *Lower Panel*: Output behavioral state over time. Special parameter value g_{57}=0.35. Please see APPENDIX 3 for other parameter values.

Also, as with the simpler system, I performed simulations to test the function of orexin in the closed-loop model. As shown in Fig. 20, the increased or decreased level of orexin affects the frequency of REM sleep and decreases or increases the number of

REM episodes correspondingly. The simulations lead to similar conclusions of the role of orexin in regulating the sleep-wake cycle for both the open-loop and closed-loop systems.

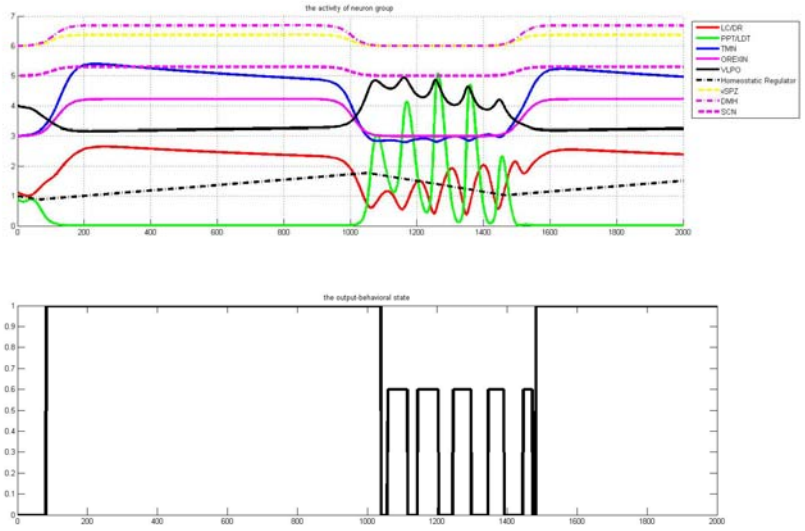

Fig. 18: Simulation result of the closed-loop two-phase model for normal sleep-wake cycle with smoothed circadian function. *Upper Panel*: Firing activity of each variable. *Lower Panel*: Output behavioral state over time. Special parameter value g_{57}=0.35. Please see APPENDIX 3 for other parameter values.

Moreover, one may test the role of the homeostatic regulator which doesn't exist in the open-loop system. This is accomplished by enlarging the effect of the homeostatic regulator, namely by increasing the parameter value g_{4s}. As Fig. 20 shows, the firing intensity of sleep-promoting neurons increases and the frequency of the NREM-REM oscillation decreases. When one decreases the effect of the homeostatic regulator, the opposite result occurs. Although no experimental results are available that would be consistent with this simulation, there are corroborating experiments [67] indicating that microinjection of adenosine can induce sleep. I simulated this phenomenon by giving the homeostatic regulator a bolus during the wake period. As shown in Fig. 21, when the bolus is large enough, the behavioral state changes from WAKE directly to SLEEP. Although the following NREM-REM oscillation is disrupted, which is possibly due to the parameter values and the simplified homeostatic function I used.

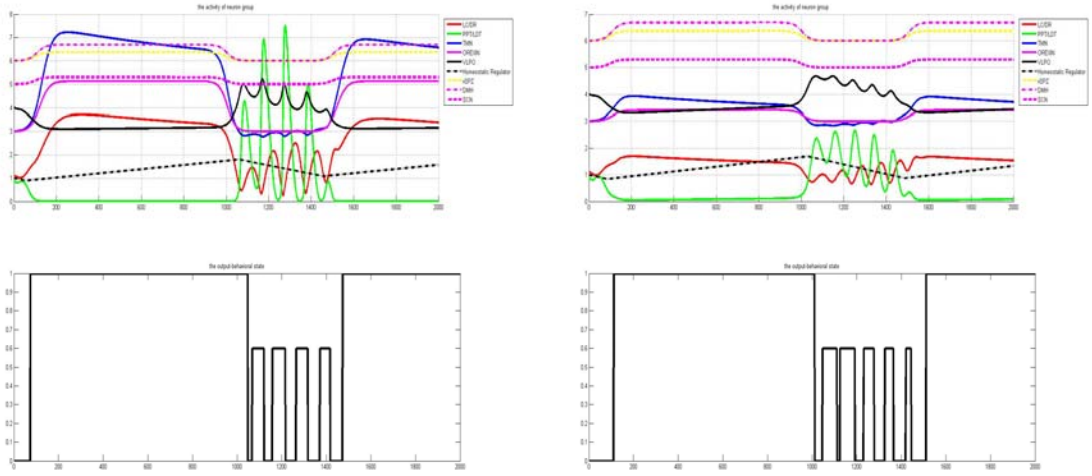

a b

Fig. 19. Simulation result of the closed-loop two-phase model for abnormal sleep-wake cycle with smoothed circadian function. (a) Result with increased level of orexin and special parameter value g_{57}=0.5; (b) Result with decreased level of orexin and special parameter value g_{57}=0.15. Each panel has two plots: the upper one shows the firing activity of each neuron group, while the lower one shows the behavioral state. Please see APPENDIX 3 for other parameter values.

To summarize this section in comparison with the open-loop system, the closed-loop system has the advantage of multilevel control and regulation of the sleep-wake cycle. Both the circadian signal and the homeostatic regulator are taken into account, although it is not possible to identify the relative importance of these two processes in the regulation of the sleep-wake cycle, either in reality or in the simulation. As the mechanisms of homeostasis and NREM-REM alternation are yet unclear, the closed-loop two-phase model still has other limitations, which are indicated by the fact that the simulation results are not exactly the same as experimental results. For example, the durations of REM episodes do not become increasingly longer in the simulation. Additionally, the values of parameters can dramatically affect the simulated results, and the choice of a set of appropriate parameter values is a challenging problem. Nevertheless, the results provide proof of principle that the modeling approach has the potential to capture the control of the sleep-wake cycle.

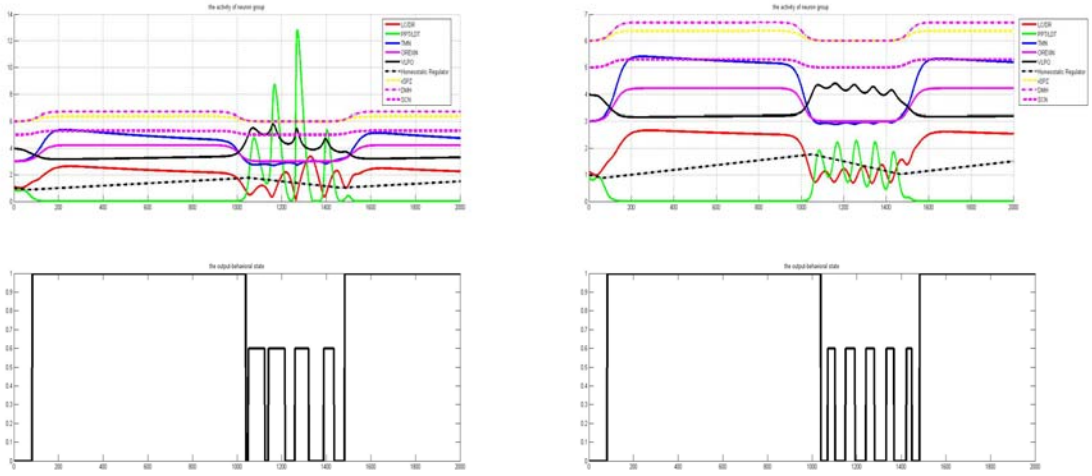

a b

Fig. 20: Simulation result of the closed-loop two-phase model for abnormal sleep-wake cycle with different homeostatic regulators. (a) Increased effect of the homeostatic regulator; special parameter value g_{4s}=0.3. (b) Decreased effect of homeostatic regulator; special parameter value g_{4s}=0.1. Each panel contains two plots. The upper one shows the firing activity of each neuron group, while the lower one shows the behavioral state. Please see APPENDIX 3 for other parameter values.

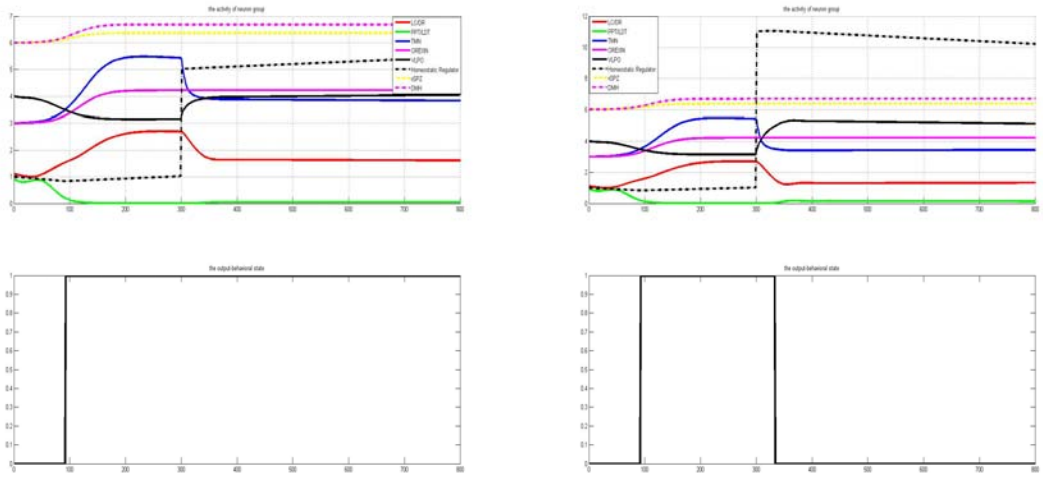

a b

Fig. 21: Simulation result of the closed-loop two-phase model upon adding a bolus of homeostatic regulator. (a) Adding a small bolus with value 2. (b) Adding a large bolus with value 5. Each panel has two plots. The upper one shows the firing activity of each neuron group, while the lower one shows the behavioral state. Please see APPENDIX 3 for other parameter values.

CHAPTER 4

FURTHER FEATURES OF THE SLEEP-WAKE CYCLE

In this chapter, I further investigate the model structure of the sleep-wake cycle, especially with respect to NREM-REM alternations, and develop a more complicated structure than the previously described simplified structure. In this fashion, the structure of the model can be made more meaningful and account for more biological details.

NREM-REM Alternation

As discussed before, NREM-REM alternations are mainly regulated by the brainstem, including the serotoninergic neurons in DR, noradrenergic neurons in LC and acetylcholinergic neurons in PPT/LDT. Recent studies have shown that some local noncholinergic neurons may also play an important intermediary role in the generation and regulation of the NREM-REM alternation. Among these neurons, a main group consists of GABAergic neurons [36, 40, 41], which can be excited by glutamatergic neurons and inhibit various wake-promoting neurons [10, 29, 33, 36, 96]. A study of the local release of GABA in dorsal raphe [30] implicates GABA release as a critical element in the production of the REM sleep state and in the control of discharge in serotonergic neurons across the sleep-wake cycle. Another group consists of glutamatergic neurons in peri-LCα. These neurons are excited by REM promoting neurons and inhibited by both wake-promoting and sleep-promoting neurons in the preoptic area [28]. Glutamatergic neurons have descending projections which are involved in muscle atonia during REM sleep [97, 98]. Mutual excitation between the cholinergic neurons and glutametergic neurons is essential for generating REM sleep [99]. Therefore, both GABAergic neurons and glutametergic neurons in the pons area can be treated as REM-promoting neurons and have a similar discharge profile [30] as REM-ON acetylcholinergic neurons in PPT/LDT.

Additionally, experimental recordings of single acetylcholine-containing neurons in PPT [24] show that there are several subtypes of neurons having different discharge profiles. Except for the REM-ON neurons, there is another main subgroup, having higher firing rates in both wakefulness and REM sleep and lower firing rate during NREM sleep. This kind of neurons can be activated by some wake-promoting neurons, such as NA in LC [100], orexin in LHA [101] and REM-promoting neurons. In contrast, the serotonergic effect on this kind of neurons has been reported to be inhibitory [100]. In order to distinguish this type of neurons from REM-ON ACH neurons, I will refer to them as "WAKE-REM-ON" (W-R-ON) ACH neurons. According to different discharge profiles and neurotransmitters, one can thus reconstruct the NREM-REM oscillating system with six components instead of the previous two. The new structure of the NREM-REM oscillating system is shown in Fig. 22.

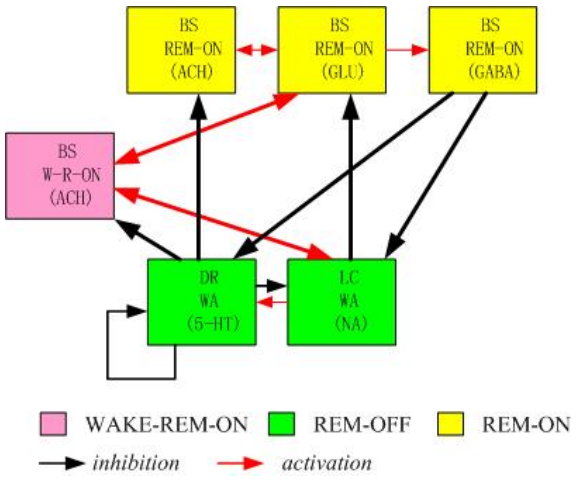

Fig. 22. Structure diagram of the NREM-REM oscillating system with six variables. Neurotransmitter and location of each neuron group are listed in the boxes.

With the model structure given in Fig. 22, it is easy to write down the corresponding S-system equations and solve them by numerical simulation. After assigning a proper set of parameter values, a preliminary simulation result of the NREM-REM oscillation is generated and shown in Fig. 23. The concrete implementation details and parameter values are given in APPENDIX 4. The simulation results show that REM-

OFF and REM-ON neurons have their firing peaks occur alternatively. As for the WAKE-REM-ON neurons, their firing peaks occur a little bit later than for the REM-ON neurons, although those two kinds of neurons should ideally have their peaks occurring simultaneously.

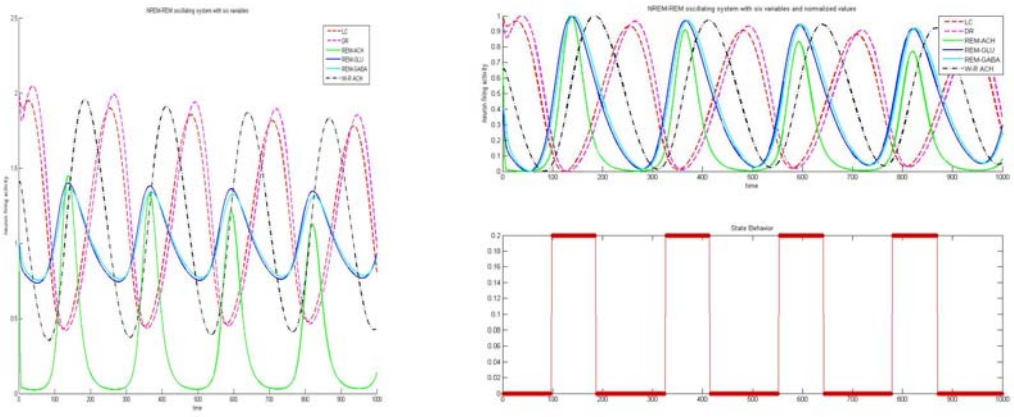

a b

Fig. 23: Preliminary simulation result of the NREM-REM oscillating system with six variables. (a) Firing activities of each neuron group with non-normalized values. (b) Firing activities of each neuron group with normalized values and the corresponding behavioral states. Please see APPENDIX 4 for parameter values and mathematical description.

In order to be able to insert this oscillating system into the comprehensive model of the sleep-wake cycle properly and to simulate how the model acts during the wake periods, an external stimulus is added to test the responses of this oscillating system. The external stimulus is considered as wake-promoting, for instance, through injection of orexin in LHA or histamine in TMN. During daytime, when the firing activity of the wake-promoting neurons is high, they would activate brainstem WAKE-REM-ON neurons and REM-OFF neurons. Three activations from this external stimulus will be separately added to WAKE-REM-ON (ACH) neurons, REM-OFF (5-HT) neurons and REM-OFF (NA) neurons. The structure diagram for adding an external stimulus is shown in Fig. 24 and the preliminary simulation results are produced as Fig. 25 shows. The external stimulus is modeled as a constant

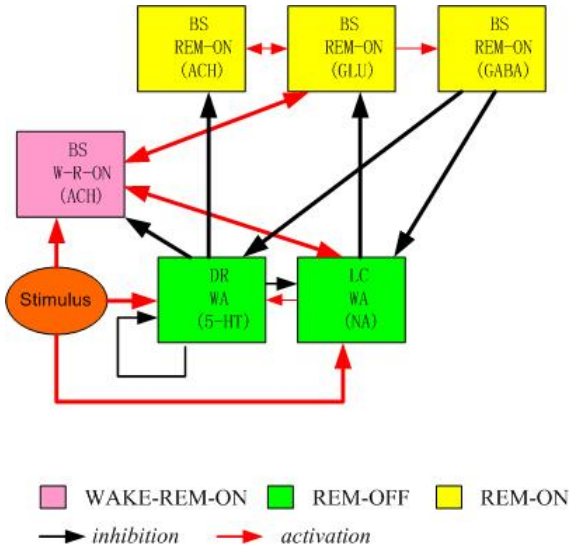

Fig. 24: Structure diagram of the NREM-REM oscillating system with six variables and an external stimulus. Neurotransmitter and location of each neuron group are listed in the boxes.

value. When its value is high (wake period), two kinds of REM-OFF neurons (LC and DR) increase their firing activity dramatically, and the REM-ON neurons decrease their firing rates and become silent. Contrary to our prediction, however, the WAKE-REM-ON neurons, which should increase their activity during wakefulness by activation from external stimulus, decrease their firing. Analysis of the model structure and parameter values used for the simulation suggests that the problem may lie with the WAKE-REM-ON neurons, which have bonds with both REM-OFF and REM-ON neurons. During sleep, the WAKE-REM-ON neurons have a discharge pattern that is more similar to REM-ON neurons than REM-OFF neurons. This guarantees that the bond between WAKE-REM-ON and REM-ON neurons is much tighter than the bond between WAKE-REM-ON and REM-OFF neurons. The external stimulus causes the REM-OFF neurons to turn on and the REM-ON neurons to turn off. Although it also activates the WAKE-REM-ON neurons, the bond between WAKE-REM-ON and REM-ON neurons is much stronger and drags the activity of WAKE-REM-ON neurons down. If one tries to weaken the bond between WAKE-REM-ON and REM-ON neurons, the original NREM-REM

alternation could be possibly disrupted and changed. A possible reason that the WAKE-REM-ON ACH neurons have high discharge rates in both wakefulness and REM sleep is that those parameters, representing the interactions between different neuron groups, may have different values during day and night time, indicating that there might be two different projecting mechanisms for WAKE-REM-ON ACH neurons during wakefulness and REM sleep. Since the biological mechanisms for NREM-REM alternation are still unclear, further experimental investigations are needed to identify the regulatory roles of each neuron group involved in the NREM-REM alternation.

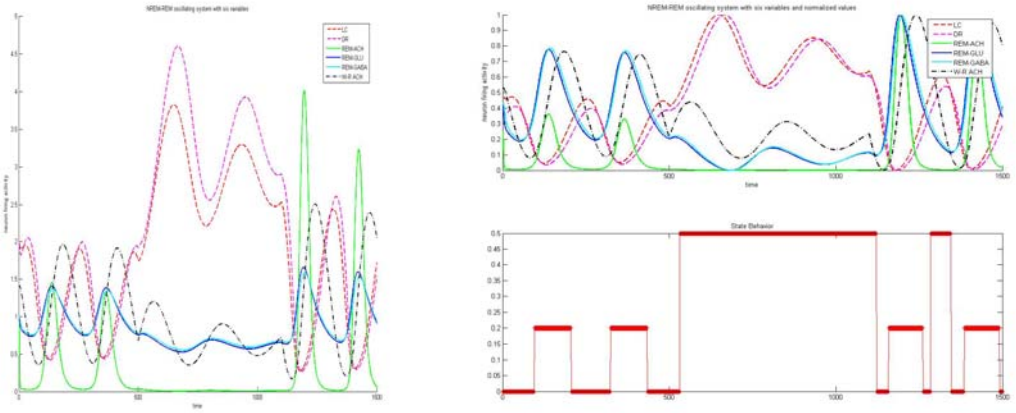

a b

Fig. 25: Preliminary simulation result of the NREM-REM oscillating system with six variables after adding stimulus. (a) Firing activities of each neuron group with non-normalized values. (b) Firing activities of each neuron group with normalized values and the corresponding behavioral states. Please see APPENDIX 4 for parameter values and mathematical formulas.

Comprehensive Structure of Sleep-Wake Cycle

As I introduce in Chapter 1, the brain stem activating system produces cortical arousal via two pathways: a dorsal route through the thalamus and a ventral route through the hypothalamus and basal forebrain. An important component for the latter route that I have not mentioned and included in the previous system is the basal forebrain (BF). The basal forebrain reportedly contains cholinergic neurons responsible for stimulating

cortical activation [102]. These cholinergic neurons are co-distributed with non-cholinergic neurons, including GABAergic neurons that could play different roles in cortical modulation and sleep-wake control [27, 103]. The diversity of the basal forebrain neurons gives rise to different efferent projections, including the cerebral cortex, posterior hypothalamus and local vicinity [103-105]. Experimental recordings of discharge properties of basal forebrain neurons [106] show several discharge patterns. Identified cholinergic neurons are found *in vivo* to discharge in rhythmic high-frequency bursts that occur with cortical activation and rhythmic theta-like EEG activity [107]. In contrast to cholinergic cells, identified GABAergic neurons are heterogeneous in their properties, but most of them discharge at higher rates in association with slow wave activity than with cortical activation [44]. Cholinergic and GABAergic neurons, as well as putative glutamatergic or peptide-containing neurons, thus possess different properties and profiles of discharge and could accordingly play different and distinctive roles in modulating cortical activity and sleep-wake control [108]. According to their discharge profiles and possible regulating roles, one could consider cholinergic neurons in BF as WAKE-REM-ON neurons and consider GABAergic neurons in BF as sleep-promoting neurons (or called NREM-REM-ON neurons) and add these two kinds of neurons into the previous model.

Several lines of evidence show that the hypothalamic preoptic area (POA) is critically implicated in the regulation of sleep. There are functionally heterogeneous cell groups with sleep-related discharge patterns located both in the medial and lateral POA. These sleep-active cells contain galanin and GABA [31, 109] and project to many components of the arousal system [31, 110]. Three distinct groups in POA can be identified as the ventrolateral preoptic nucleus (VLPO), the extended ventrolateral preoptic nucleus (eVLPO) and the median preoptic nucleus (MnPN). Although they have similar anatomical, physiological and neurochemical properties, these three areas may have distinct roles in regulating sleep-wake states. A lesion study [37] has shown that the

VLPO cluster is a necessary component of the sleep circuitry, without which NREM sleep is severely impaired, while lesions in the region of eVLPO caused smaller changes in NREM sleep time. And further study [28] showed that the extended VLPO is highly correlated with REM sleep but not NREM sleep. A discharge pattern study [25] indicated MnPN neurons that progressively increase activity during sustained waking and decrease activity during sustained sleep states may be involved in homeostatic regulation of sleep. Further homeostasis studies [111, 112] show that the elevated homeostatic pressure for NREM and REM sleep can be associated with increased activity of subsets of MnPN and VLPO neurons. Experimental results indicate that MnPN GABAergic neurons are most strongly activated in response to increasing sleep pressure, whereas VLPO GABAergic neurons are most strongly activated in response to increasing sleep amount, which indicates their different roles in homeostatic aspects of sleep regulation. Moreover, unlike neurons in VLPO, neurons in MnPN are reported [113] to be among the strongest sources of projections to lateral hypothalamic area. Taken all these considerations into account, it is useful to treat the three sleep-active nuclei separately in order to identify their distinctive regulating roles in sleep-wake cycle most clearly.

Combining all these biological considerations leads to a more comprehensive structure of the sleep-wake cycle, as shown in Fig. 26. The circadian rhythm is still considered as a 24-hour periodic external signal. The big blue open brace indicates that the behavioral states recorded in the cortex are determined by firing activities of all underlying neuron groups. The homeostatic regulator changes according to different states and affects the sleep-promoting components and cholinergic neurons in basal forebrain as a “feedback regulator”. Different colors of the boxes mean different areas of the brain. The arrows represent identified or hypothesized interactions between different neurons groups. Neurons groups are identified and separated according to their different locations, neurotransmitters and possible regulating roles.

Due to the difficulty of finding a set of appropriate parameter values to make the whole system work properly, I have not yet implemented this system. Nonetheless, the discussion of earlier structures and their translation into S-system models demonstrate that a model formulation of this more comprehensive model would be possible and how it would be achieved. With an increasing amount of specific physiological and biological findings, it will be possible to update and revise the structure of the current system and it is to be expected that a more realistic model structure of the sleep-wake cycle will emerge and that factors at different levels, such as the gene regulation and thalamic oscillator, should be included in future models.

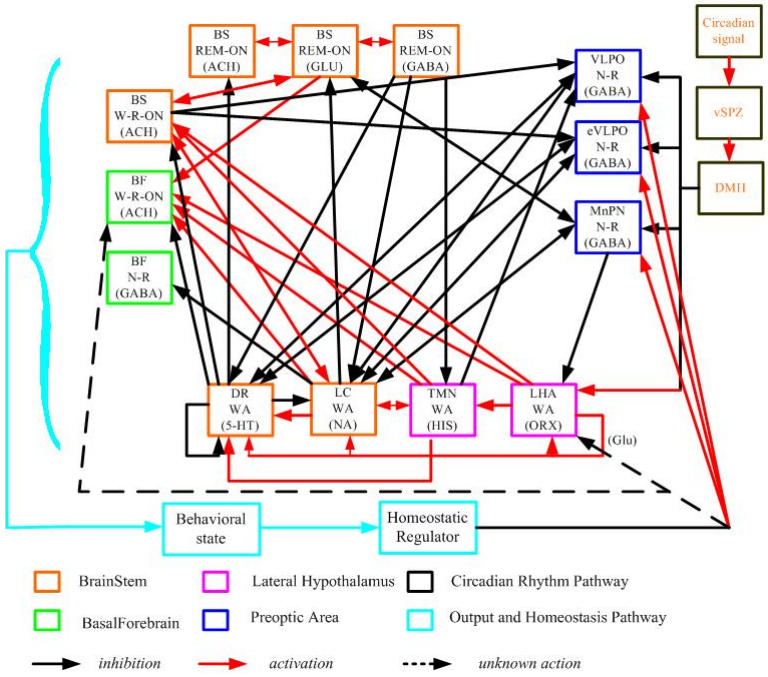

Fig. 26: More comprehensive structure diagram of the sleep-wake cycle. Different colors of boxes represent different regulating roles and different locations. Neurotransmitters and the corresponding discharge category of each neuron group are listed in box. Unlike red and black lines, blue lines do not represent the projections between neuron groups, but show positive or negative relationships between two connected objects.

CHAPTER 5

CONCLUSIONS AND FUTURE RESEARCH DIRECTIONS

This thesis proposes a two-phase model for the sleep-wake cycle. Using the S-system method, both open-loop and closed-loop forms of the model are translated into a set of corresponding ordinary differential equations and implemented in MATLAB. From the simulation results shown in the above chapters, we can see that the two-phase model can achieve some features of the sleep-wake cycle. It has the capability of simulating basic firing activities of neuron groups and behavioral states switching during the normal sleep-wake periods, or testing the role of neuropeptide (orexin) and homeostatic regulator in the abnormal sleep-wake cycle. However, the model still has a few limitations. First, both the open-loop and closed-loop forms of the two-phase model are only implemented on the simplified version of the model structure. Some special features of the firing activity for certain neuron groups can not be shown by either of these two forms. For example, the WAKE-REM-ON acetylcholine-containing neurons discussed in Chapter 4 are not included in either of these two forms. Additionally, how to choose appropriate parameter values is a considerable challenge for implementation. The achievements and limitations of both open-loop and close-loop forms of the two-phase model are summarized in the Table 2 and Table 3.

Future research should continue to focus on the analysis of more comprehensive and complicated model structures of the sleep-wake cycle. Efforts should be invested in the following directions:

1. Clarify the role of each kind of neuron group in NREM-REM alternations
2. Consider to use more reasonable functions to model the homeostatic regulator
3. Implement the sleep-wake cycle system with a more comprehensive model structure
4. Use actual data to obtain reliable parameter values for the models.

Table 2. Achievements and limitations of the open-loop two-phase model.

	Achievements	Limitations
Open-loop form	• basic firing activity of most neuron groups • behavioral state switching during the sleep-wake cycle • one controlling process • testing role of orexin	• Durations of REM episodes are all of the same length • Other control factors are needed to be included • Firing activities of some neuron groups (*i.e.*, serotonin or orexin), remain unchanged during the sleep period • Only the simplified model structure has been implemented

Table 3. Achievements and limitations of the closed-loop two-phase model.

	Achievements	Limitations
Closed-loop form	• basic firing activity of most neuron groups • behavioral states switching during the sleep-wake cycle • two controlling processes • testing role of orexin • testing role of homeostatic regulator • firing activity of some neuron group (*i.e.*, serotonin) don't keep constant during sleep period	• Durations of REM episodes are not the same as experimental observations • Implementations are done only on simplified model structure • Firing activity of orexin neuron is not completely consistent with the experimental results • Parameter values choosing will dramatically affect the simulation result

APPENDIX 1

IMPLEMENTATION OF BASIC ACTION TESTING

The activation and inhibition test with the S-system method is implemented in MATLAB. The values of the input signal and the corresponding parameters in equation (2) are given by:

$$\alpha = [1.3 \quad 1.2]; \quad \beta = [1 \quad 1];$$

$$g = \begin{bmatrix} -0.5 & 0.2 \\ 0.3 & -0.2 \end{bmatrix}; \quad h = \begin{bmatrix} 0.3 & 0 \\ 0 & 0.35 \end{bmatrix}$$

$$S_1 = \begin{cases} 2, & 0 \le t < 100 \\ 1, & others \end{cases}$$

$$S_2 = \begin{cases} 2, & 200 \le t < 300 \\ 1, & else \end{cases}$$

The self-action test with the S-system method is also implemented in MATLAB. The values of the input signal and the corresponding parameters in equation (3) are given by:

$$self - activation:$$

$$\alpha_1 = \beta_1 = 1; \quad g_{1s} = 0.3; \quad g_{11} = 0.2; \quad h_{11} = 0.25;$$

$$self - inhibition:$$

$$\alpha_1 = \beta_1 = 1; \quad g_{1s} = 0.3; \quad g_{11} = -0.2; \quad h_{11} = 0.25;$$

$$external - input:$$

$$S_1 = \begin{cases} 2, & 0 \le t < 100 \\ 1, & else \end{cases}$$

For the comparative simulation of a system without self-action, the values of the input signal and the parameters are the same except that the value of g_{11} is zero.

APPENDIX 2

IMPLEMENTATION OF THE OPEN-LOOP TWO-PHASE MODEL

The simplified version of the open-loop two-phase model of the sleep-wake cycle with the corresponding system equations (4) is implemented in MATLAB. The parameter values of the preliminary results (shown in Fig.12) are given as follows:

$$\alpha = [1.962 \quad 1.96 \quad 1.8 \quad 2.5 \quad 1 \quad 1 \quad 1];$$

$$\beta = [1.962 \quad 1.96 \quad 1 \quad 1 \quad 1 \quad 1 \quad 1];$$

$$g = \begin{bmatrix} -0.09194 & -0.01346 & 0 & -0.0001 & 0.008 & 0 & 0 \\ -0.1991 & 0.44191 & 0 & 0 & 0.003 & 0 & 0 \\ 0 & 0 & 0 & -0.3 & 0.4 & 0 & 0 \\ -0.005 & 0 & -0.3 & 0 & 0 & 0 & -0.2 \\ 0 & 0 & 0 & 0 & 0 & 0 & 0.2 \\ 0 & 0 & 0 & 0 & 0 & 0 & 0 \\ 0 & 0 & 0 & 0 & 0 & 0.5 & 0 \end{bmatrix};$$

$$h = \begin{bmatrix} -0.13462 & 0 & 0 & 0 & 0 & 0 & 0 \\ 0 & 0.486709 & 0 & 0 & 0 & 0 & 0 \\ 0 & 0 & 0.6 & 0 & 0 & 0 & 0 \\ 0 & 0 & 0 & 0.6 & 0 & 0 & 0 \\ 0 & 0 & 0 & 0 & 0.5 & 0 & 0 \\ 0 & 0 & 0 & 0 & 0 & 0.6 & 0 \\ 0 & 0 & 0 & 0 & 0 & 0 & 0.5 \end{bmatrix};$$

$$g_{6s} = 1.393 \ ;$$

For the abnormal case of the sleep-wake cycle shown in Figs. 13 a and b, only the value of parameter g_{57} is changed as indicated in the description below the figure. Other parameter values are unchanged.

The circadian signal is modeled as a step function with the following settings:

$$SCN = \begin{cases} 2, & 0 \le t < 960, \text{ or } 1440 \le t < 2400; \\ 1, & 960 \le t < 1440, \text{ or } 2440 \le t < 2880; \end{cases}$$

Additionally, the behavioral state is defined by the following criteria:

$$State = \begin{cases} 1, & (X_4 > 1.5) \,\&\, (X_1 > 0.6) \\ 0.6, & X_2 > 0.4 \\ 0, & else \end{cases}$$

where 1, 0.6 and 0 respectively represent the WAKE, REM and NREM states.

APPENDIX 3

IMPLEMENTATION OF THE CLOSED-LOOP TWO-PHASE MODEL

The simplified version of the closed-loop two-phase model of the sleep-wake cycle with the corresponding system (10) is implemented in MATLAB. The parameter values of the preliminary results (shown in Figs. 17 and 18) are given as:

$$\alpha = [0.152 \quad 0.15 \quad 1 \quad 1 \quad 1 \quad 1 \quad 1];$$

$$\beta = [0.152 \quad 0.15 \quad 1 \quad 1 \quad 1 \quad 1 \quad 1];$$

$$g = \begin{bmatrix} -0.61 & 0.26 & 0.4 & -0.2 & 0.6 & 0 & 0 \\ -1.2 & 0.2531 & 0 & -0.05 & 0 & 0 & 0 \\ 0 & 0 & 0 & -0.15 & 0.35 & 0 & 0 \\ -0.08 & 0 & -0.3 & 0 & 0 & 0 & -0.2 \\ 0 & 0 & 0 & 0 & 0 & 0 & 0.35 \\ 0 & 0 & 0 & 0 & 0 & 0 & 0 \\ 0 & 0 & 0 & 0 & 0 & 0.5 & 0 \end{bmatrix};$$

$$h = \begin{bmatrix} -0.714 & 0 & 0 & 0 & 0 & 0 & 0 \\ 0 & 0.45 & 0 & 0 & 0 & 0 & 0 \\ 0 & 0 & 0.45 & 0 & 0 & 0 & 0 \\ 0 & 0 & 0 & 0.3 & 0 & 0 & 0 \\ 0 & 0 & 0 & 0 & 0.23 & 0 & 0 \\ 0 & 0 & 0 & 0 & 0 & 0.5 & 0 \\ 0 & 0 & 0 & 0 & 0 & 0 & 0.3 \end{bmatrix};$$

$$g_{4s} = 0.2; \quad g_{6s} = 0.6$$

For other abnormal cases and for testing case simulations shown in Figs. 19, 20 and 21, all parameters remained the same as above except for those indicated in the figure legend.

The external circadian signals shown in Fig. 16 are modeled with two different functions; one is a step function defined as

$$SCN = \begin{cases} 2, & 100 \le t < 1000, \, or \, 1500 \le t < 1800; \\ 1, & 0 \le t < 100, \, or \, 1000 \le t < 1500; \end{cases}$$

The other signal is modeled as a smoothed step function. The mathematical specifications are:

$$SCN = \begin{cases} \dfrac{0.3}{1+\exp(-0.05*(t-100))}+1, & 0 \le t < 900; \\ \dfrac{0.3}{1+\exp(-0.05*(1000-t))}+1, & 900 \le t < 1400; \\ \dfrac{0.3}{1+\exp(-0.05*(t-1500))}+1, & 1400 \le t < 1800; \end{cases}$$

The homeostatic regulator X_9 is modeled with an ordinary differential equation (11) without noise as:

$$\dot{X}_9 = 0.9*(0.001*\delta_{wake} - 0.02*\delta_{sleep}) + 0$$

Moreover, the behavioral state is defined by the following criteria:

$$State = \begin{cases} 1, & (X_3 > 1.3) \\ 0.6, & (X_2 > 1.5) \\ 0, & else \end{cases}$$

where 1, 0.6 and 0 respectively represents the WAKE, REM and NREM states.

APPENDIX 4

IMPLEMENTATION OF NREM-REM OSCILLATIONS WITH SIX-VARIABLES

The S-system equations for the NREM-REM oscillating system with six variables (model structure shown in Fig. 22) are given as

$$\dot{X}_1 = \alpha_1 X_2^{g_{12}} X_5^{g_{15}} X_6^{g_{16}} - \beta_1 X_1^{h_{11}}$$
$$\dot{X}_2 = \alpha_2 X_1^{g_{21}} X_2^{g_{22}} X_5^{g_{25}} - \beta_2 X_2^{h_{22}}$$
$$\dot{X}_3 = \alpha_3 X_2^{g_{32}} X_4^{g_{34}} - \beta_3 X_3^{h_{11}}$$
$$\dot{X}_4 = \alpha_4 X_1^{g_{41}} X_3^{g_{43}} X_6^{g_{46}} - \beta_4 X_4^{h_{44}}$$
$$\dot{X}_5 = \alpha_5 X_4^{g_{54}} - \beta_5 X_5^{h_{55}}$$
$$\dot{X}_6 = \alpha_6 X_1^{g_{61}} X_2^{g_{62}} X_4^{g_{64}} - \beta_6 X_6^{h_{66}}$$

where $X_1 \cdots X_6$ represents the neuron groups in LC (NA), DR (5-HT), BS (REM-ON ACH), BS (REM-ON GLU), BS (REM-ON GABA) and BS (W-R-ON ACH). The parameter values for the preliminary simulation results shown in Fig. 23 are given as

$$\alpha = [0.3 \quad 0.3 \quad 0.3 \quad 0.3 \quad 0.3 \quad 0.1575];$$
$$\beta = [0.3 \quad 0.3 \quad 0.6 \quad 0.3 \quad 0.3 \quad 0.1575];$$
$$g = \begin{bmatrix} 0 & -0.15 & 0 & 0 & 0.18 & -0.64 & 0.18 \\ 0.93 & -0.67 & 0 & 0 & -0.82 & 0 \\ 0 & -0.71 & 0 & 0.7 & 0 & 0 \\ -0.32 & 0 & 0.001 & 0 & 0 & 0.11 \\ 0 & 0 & 0 & 0.71 & 0 & 0 \\ 0.31 & -0.11 & 0 & 1 & 0 & 0 \end{bmatrix};$$
$$h = \begin{bmatrix} 0.06 & 0 & 0 & 0 & 0 & 0 \\ 0 & 0.47 & 0 & 0 & 0 & 0 \\ 0 & 0 & 0.38 & 0 & 0 & 0 \\ 0 & 0 & 0 & 0.79 & 0 & 0 \\ 0 & 0 & 0 & 0 & 0.77 & 0 \\ 0 & 0 & 0 & 0 & 0 & 0.2 \end{bmatrix}$$

The behavioral states are defined by the following criteria:

$$State = \begin{cases} 1, & (X_1 > 0.5); \\ 0.6, & (X_4 \geq 0.4) \,\&\, (X_1 < 0.35); \\ 0, & else \end{cases}$$

where 1, 0.6 and 0 respectively represent the WAKE, REM and NREM states, and the quantities used here are normalized values.

The S-system equations for the NREM-REM oscillating system with six variables and an external stimulus (with model structure shown in Fig. 24) are

$$\begin{aligned}
\dot{X}_1 &= \alpha_1 X_2^{g_{12}} X_5^{g_{15}} X_6^{g_{16}} [S]^{g_{1s}} - \beta_1 X_1^{h_{11}} \\
\dot{X}_2 &= \alpha_2 X_1^{g_{21}} X_2^{g_{22}} X_5^{g_{25}} [S]^{g_{2s}} - \beta_2 X_2^{h_{22}} \\
\dot{X}_3 &= \alpha_3 X_2^{g_{32}} X_4^{g_{34}} - \beta_3 X_3^{h_{11}} \\
\dot{X}_4 &= \alpha_4 X_1^{g_{41}} X_3^{g_{43}} X_6^{g_{46}} - \beta_4 X_4^{h_{44}} \\
\dot{X}_5 &= \alpha_5 X_4^{g_{54}} - \beta_5 X_5^{h_{55}} \\
\dot{X}_6 &= \alpha_6 X_1^{g_{61}} X_2^{g_{62}} X_4^{g_{64}} [S]^{g_{6s}} - \beta_6 X_6^{h_{66}}
\end{aligned}$$

where *S* represents the external stimulus and all other variables have the same meaning as above.

All parameters have the same values shown above. The values of the newly added parameters are given by:

$$g_{1s} = 0.05; \quad g_{2s} = 0.05; \quad g_{3s} = 0.3$$

The external stimulus is modeled as a stepwise function as:

$$S = \begin{cases} 2, & 500 \leq t < 1100 \\ 1, & else \end{cases}$$

The simulation is run for 1000 minutes for the system without external stimulus and for 1500 minutes for the system with external stimulus.

REFERENCES

1. Sinton, C.M. and R.W. McCarley, *Neurophysiological mechanisms of sleep and wakefulness: a question of balance.* Semin Neurol, 2004. **24**(3): p. 211-23.

2. Siegel, J.M., *Narcolepsy: a key role for hypocretins (orexins).* Cell, 1999. **98**(4): p. 409-12.

3. Chemelli, R.M., et al., *Narcolepsy in orexin knockout mice: molecular genetics of sleep regulation.* Cell, 1999. **98**(4): p. 437-51.

4. Lin, L., et al., *The sleep disorder canine narcolepsy is caused by a mutation in the hypocretin (orexin) receptor 2 gene.* Cell, 1999. **98**(3): p. 365-76.

5. Siegel, J., *Brain mechanisms that control sleep and waking.* Naturwissenschaften, 2004. **91**(8): p. 355-65.

6. Jones, B.E., *From waking to sleeping: neuronal and chemical substrates.* Trends Pharmacol Sci, 2005. **26**(11): p. 578-86.

7. Siegel, J.M., *The neurotransmitters of sleep.* J Clin Psychiatry, 2004. **65 Suppl 16**: p. 4-7.

8. Sakai, K., *Physiological properties and afferent connections of the locus coeruleus and adjacent tegmental neurons involved in the generation of paradoxical sleep in the cat.* Prog Brain Res, 1991. **88**: p. 31-45.

9. Kilduff, T.S. and C. Peyron, *The hypocretin/orexin ligand-receptor system: implications for sleep and sleep disorders.* Trends Neurosci, 2000. **23**(8): p. 359-65.

10. Nitz, D. and J.M. Siegel, *GABA release in the locus coeruleus as a function of sleep/wake state.* Neuroscience, 1997. **78**(3): p. 795-801.

11. McCarley, R.W., et al., *Brainstem neuromodulation and REM sleep.* the neurosciences, 1995. **7**: p. 341-354.

12. Wu, M.F., et al., *Locus coeruleus neurons: cessation of activity during cataplexy.* Neuroscience, 1999. **91**(4): p. 1389-99.

13. Wu, M.F., et al., *Activity of dorsal raphe cells across the sleep-waking cycle and during cataplexy in narcoleptic dogs.* J Physiol, 2004. **554**(Pt 1): p. 202-15.

14. Beuckmann, C.T. and M. Yanagisawa, *Orexins: from neuropeptides to energy homeostasis and sleep/wake regulation.* J Mol Med, 2002. **80**(6): p. 329-42.

15. John, J., et al., *Cataplexy-active neurons in the hypothalamus: implications for the role of histamine in sleep and waking behavior.* Neuron, 2004. **42**(4): p. 619-34.

16. Yamanaka, A., et al., *Orexins activate histaminergic neurons via the orexin 2 receptor.* Biochem Biophys Res Commun, 2002. **290**(4): p. 1237-45.

17. Sakurai, T., et al., *Orexins and orexin receptors: a family of hypothalamic neuropeptides and G protein-coupled receptors that regulate feeding behavior.* Cell, 1998. **92**(5): p. 1 page following 696.

18. de Lecea, L. and J.G. Sutcliffe, *The hypocretins and sleep.* Febs J, 2005. **272**(22): p. 5675-88.

19. Li, Y., et al., *Hypocretin/Orexin excites hypocretin neurons via a local glutamate neuron-A potential mechanism for orchestrating the hypothalamic arousal system.* Neuron, 2002. **36**(6): p. 1169-81.

20. Sutcliffe, J.G. and L. de Lecea, *The hypocretins: excitatory neuromodulatory peptides for multiple homeostatic systems, including sleep and feeding.* J Neurosci Res, 2000. **62**(2): p. 161-8.

21. Sakurai, T., *Orexin: a link between energy homeostasis and adaptive behaviour.* Curr Opin Clin Nutr Metab Care, 2003. **6**(4): p. 353-60.

22. Mileykovskiy, B.Y., L.I. Kiyashchenko, and J.M. Siegel, *Behavioral correlates of activity in identified hypocretin/orexin neurons.* Neuron, 2005. **46**(5): p. 787-98.

23. Lee, M.G., et al., *Cholinergic basal forebrain neurons burst with theta during waking and paradoxical sleep.* J Neurosci, 2005. **25**(17): p. 4365-9.

24. Datta, S. and D.F. Siwek, *Single Cell Activity Patterns of Pedunculopontine Tegmentum Neurons Across the Sleep-Wake Cycle in the Freely Moving Rats.* Journal of Neuroscience Research, 2002. **70**: p. 611-621.

25. Suntsova, N., et al., *Sleep-waking discharge patterns of median preoptic nucleus neurons in rats.* J Physiol, 2002. **543**(Pt 2): p. 665-77.

26. Szymusiak, R., et al., *Sleep-waking discharge patterns of ventrolateral preoptic/anterior hypothalamic neurons in rats.* Brain Res, 1998. **803**(1-2): p. 178-88.

27. Gritti, I., L. Mainville, and B.E. Jones, *Codistribution of GABA- with acetylcholine-synthesizing neurons in the basal forebrain of the rat.* J Comp Neurol, 1993. **329**(4): p. 438-57.

28. Lu, J., et al., *Selective Activation of the Extended Ventrolateral preoptic Nucleus during Rapid Eye Movement Sleep.* The Journal of Neuroscience, 2002. **22**(11): p. 4568-4576.

29. Nitz, D. and J.M. Siegel, *GABA release in posterior hypothalamus across sleep-wake cycle.* Am J Physiol, 1996. **271**(6 Pt 2): p. R1707-12.

30. Nitz, D. and J. Siegel, *GABA release in the dorsal raphe nucleus: role in the control of REM sleep.* Am J Physiol, 1997. **273**(1 Pt 2): p. R451-5.

31. Sherin, J.E., et al., *Innervation of Histaminergic Tuberomammillary Neurons by GABAergic and Galaninergic Neurons in the Ventrolateral Preoptic Nucleus of the Rat.* The Journal of Neuroscience, 1998. **18**(12): p. 4705-4721.

32. Henny, P. and B.E. Jones, *Innervation of orexin/hypocretin neurons by GABAergic, glutamatergic or cholinergic basal forebrain terminals evidenced by immunostaining for presynaptic vesicular transporter and postsynaptic scaffolding proteins.* J Comp Neurol, 2006. **499**(4): p. 645-61.

33. Mallick, B.N., S. Kaur, and R.N. Saxena, *Interactions between cholinergic and GABAergic neurotransmitters in and around the locus coeruleus for the induction and maintenance of rapid eye movement sleep in rats.* Neuroscience, 2001. **104**(2): p. 467-85.

34. Sakai, K. and S. Crochet, *Serotonergic dorsal raphe neurons cease firing by disfacilitation during paradoxical sleep.* Neuroreport, 2000. **11**(14): p. 3237-41.

35. Verret, L., et al., *Cholinergic and noncholinergic brainstem neurons expressing Fos after paradoxical (REM) sleep deprivation and recovery.* Eur J Neurosci, 2005. **21**(9): p. 2488-504.

36. Maloney, K.J., L. Mainville, and B.E. Jones, *Differential c-Fos expression in cholinergic, monoaminergic, and GABAergic cell groups of the pontomesencephalic tegmentum after paradoxical sleep deprivation and recovery.* J Neurosci, 1999. **19**(8): p. 3057-72.

37. Lu, J., et al., *Effect of lesions of the ventrolateral preoptic nucleus on NREM and REM sleep.* J Neurosci, 2000. **20**(10): p. 3830-42.

38. Pal, D. and B.N. Mallick, *GABA in pedunculo pontine tegmentum regulates spontaneous rapid eye movement sleep by acting on GABAA receptors in freely moving rats.* Neurosci Lett, 2004. **365**(3): p. 200-4.

39. Vazquez, J. and H.A. Baghdoyan, *GABAA receptors inhibit acetylcholine release in cat pontine reticular formation: implications for REM sleep regulation.* J Neurophysiol, 2004. **92**(4): p. 2198-206.

40. Torterolo, P., F.R. Morales, and M.H. Chase, *GABAergic mechanisms in the pedunculopontine tegmental nucleus of the cat promote active (REM) sleep.* Brain Res, 2002. **944**(1-2): p. 1-9.

41. Torterolo, P., et al., *GABAergic neurons of the laterodorsal and pedunculopontine tegmental nuclei of the cat express c-fos during carbachol-induced active sleep.* Brain Res, 2001. **892**(2): p. 309-19.

42. Xi, M.C., F.R. Morales, and M.H. Chase, *Interactions between GABAergic and cholinergic processes in the nucleus pontis oralis: neuronal mechanisms controlling active (rapid eye movement) sleep and wakefulness.* J Neurosci, 2004. **24**(47): p. 10670-8.

43. Pal, D. and B.N. Mallick, *Role of noradrenergic and GABA-ergic inputs in pedunculopontine tegmentum for regulation of rapid eye movement sleep in rats.* Neuropharmacology, 2006. **51**(1): p. 1-11.

44. Manns, I.D., A. Alonso, and B.E. Jones, *Discharge profiles of juxtacellularly labeled and immunohistochemically identified GABAergic basal forebrain neurons recorded in association with the electroencephalogram in anesthetized rats.* J Neurosci, 2000. **20**(24): p. 9252-63.

45. Saper, C.B., T.E. Scammell, and J. Lu, *Hypothalamic regulation of sleep and circadian rhythms.* Nature, 2005. **437**(7063): p. 1257-63.

46. Moore, R.Y. and V.B. Eichler, *Loss of a circadian adrenal corticosterone rhythm following suprachiasmatic lesions in the rat.* Brain Res, 1972. **42**(1): p. 201-6.

47. Mistlberger, R.E., *Circadian regulation of sleep in mammals: role of the suprachiasmatic nucleus.* Brain Res Brain Res Rev, 2005. **49**(3): p. 429-54.

48. Saper, C.B., et al., *The hypothalamic integrator for circadian rhythms.* trends Neurosci, 2005. **28**(3): p. 152-157.

49. Deurveilher, S., J. Burns, and K. Semba, *Indirect projections from the suprachiasmatic nucleus to the ventrolateral preoptic nucleus: a dual tract-tracing study in rat.* Eur J Neurosci, 2002. **16**(7): p. 1195-213.

50. Deurveilher, S. and K. Semba, *Indirect projections from the suprachiasmatic nucleus to the median preoptic nucleus in rat.* Brain Res, 2003. **987**(1): p. 100-6.

51. Sakurai, T., et al., *Input of orexin/hypocretin neurons revealed by a genetically encoded tracer in mice.* Neuron, 2005. **46**(2): p. 297-308.

52. Yoshida, K., et al., *Afferents to the orexin neurons of the rat brain.* J Comp Neurol, 2006. **494**(5): p. 845-61.

53. Deurveilher, S. and K. Semba, *Indirect projections from the suprachiasmatic nucleus to major arousal-promoting cell groups in rat: implications for the circadian control of behavioural state.* Neuroscience, 2005. **130**(1): p. 165-83.

54. Lu, J., et al., *Contrasting effects of ibotenate lesions of the paraventricular nucleus and subparaventricular zone on sleep-wake cycle and temperature regulation.* J Neurosci, 2001. **21**(13): p. 4864-74.

55. Chou, T.C., et al., *Afferents to the ventrolateral preoptic nucleus.* J Neurosci, 2002. **22**(3): p. 977-90.

56. Aston-Jones, G., et al., *A neural circuit for circadian regulation of arousal.* Nat Neurosci, 2001. **4**(7): p. 732-8.

57. Chou, T.C., et al., *Critical role of dorsomedial hypothalamic nucleus in a wide range of behavioral circadian rhythms.* J Neurosci, 2003. **23**(33): p. 10691-702.

58. Borbely, A.A., *A two process model of sleep regulation.* Hum Neurobiol, 1982. **1**(3): p. 195-204.

59. Porkka-Heiskanen, T., et al., *Adenosine and sleep.* Sleep Med Rev, 2002. **6**(4): p. 321-32.

60. Basheer, R., et al., *Adenosine and sleep-wake regulation.* Prog Neurobiol, 2004. **73**(6): p. 379-96.

61. Porkka-Heiskanen, T., *Adenosine in sleep and wakefulness.* Ann Med, 1999. **31**(2): p. 125-9.

62. Porkka-Heiskanen, T., et al., *Adenosine, energy metabolism, and sleep.* ScientificWorldJournal, 2003. **3**: p. 790-8.

63. McGinty, D. and R. Szymusiak, *Brain structures and mechanisms involved in the generation of NREM sleep: focus on the preoptic hypothalamus.* Sleep Med Rev, 2001. **5**(4): p. 323-342.

64. Hayaishi, O. and Y. Urade, *Prostaglandin D2 in sleep-wake regulation: recent progress and perspectives.* Neuroscientist, 2002. **8**(1): p. 12-5.

65. Hayaishi, O., *Molecular genetic studies on sleep-wake regulation, with special emphasis on the prostaglandin D(2) system.* J Appl Physiol, 2002. **92**(2): p. 863-8.

66. Noor Alam, M.D., R. Szymusiak, and D. McGinty, *Adenosinergic regulation of sleep: multiple sites of action in the brain.* Sleep, 2006. **29**(11): p. 1384-5; discussion 1387-9.

67. Porkka-Heiskanen, T., et al., *Adenosine: a mediator of the sleep-inducing effects of prolonged wakefulness.* Science, 1997. **276**(5316): p. 1265-8.

68. Strecker, R.E., et al., *Adenosinergic modulation of basal forebrain and preoptic/anterior hypothalamic neuronal activity in the control of behavioral state.* Behav Brain Res, 2000. **115**(2): p. 183-204.

69. Scammell, T.E., et al., *An adenosine A2a agonist increases sleep and induces Fos in ventrolateral preoptic neurons.* Neuroscience, 2001. **107**(4): p. 653-63.

70. Borbely, A.A. and P. Achermann, *Sleep homeostasis and models of sleep regulation.* J Biol Rhythms, 1999. **14**(6): p. 557-68.

71. Saper, C.B., T.C. Chou, and T.E. Scammell, *The sleep switch: hypothalamic control of sleep and wakefulness.* Trends Neurosci, 2001. **24**(12): p. 726-31.

72. Pace-Schott, E.F. and J.A. Hobson, *The neurobiology of sleep: genetics, cellular physiology and subcortical networks.* Nat Rev Neurosci, 2002. **3**(8): p. 591-605.

73. McGinty, D.J. and R.R. Drucker-Colin, *Sleep mechanisms: biology and control of REM sleep.* Int Rev Neurobiol, 1982. **23**: p. 391-436.

74. Pace-Schott, E.F. and J.A. Hobson, *Basic Mechanisms of Sleep: New Evidence on the Neuroanotomy and Neuromodulation of the NREM-REM Cycle.* neuropsychopharmacology: the fifth generation of progress, 2001. **128**: p. 1859-1877.

75. Lu, J., et al., *A putative flip-flop switch for control of REM sleep.* Nature, 2006. **441**(7093): p. 589-94.

76. Hobson, J.A., R.W. McCarley, and P.W. Wyzinski, *Sleep cycle oscillation: reciprocal discharge by two brainstem neuronal groups.* Science, 1975. **189**(4196): p. 55-8.

77. McCarley, R.W. and J.A. Hobson, *Neuronal excitability modulation over the sleep cycle: a structural and mathematical model.* Science, 1975. **189**(4196): p. 58-60.

78. McCarley, R.W. and S.G. Massaquoi, *A limit cycle mathematical model of the REM sleep oscillator system.* Am J Physiol, 1986. **251**(6 Pt 2): p. R1011-29.

79. Achermann, P. and A.A. Borbely, *Mathematical models of sleep regulation.* Front Biosci, 2003. **8**: p. s683-93.

80. Achermann, P., et al., *A model of human sleep homeostasis based on EEG slow-wave activity: quantitative comparison of data and simulations.* Brain Res Bull, 1993. **31**(1-2): p. 97-113.

81. Tamakawa, Y., et al., *A quartet neural system model orchestrating sleep and wakefulness mechanisms.* J Neurophysiol, 2006. **95**(4): p. 2055-69.

82. Voit, E.O., *Symmetries of S-systems.* Math Biosci, 1992. **109**(1): p. 19-37.

83. O.Voit, E., *Computational Analysis of Biochemical Systems-A Pratical Guide for Biochemists and Molecular Biologists.* 2000.

84. Steininger, T.L., et al., *Sleep-waking discharge of neurons in the posterior lateral hypothalamus of the albino rat.* Brain Res, 1999. **840**(1-2): p. 138-47.

85. Guzman-Marin, R., et al., *Discharge modulation of rat dorsal raphe neurons during sleep and waking: effects of preoptic/basal forebrain warming.* Brain Res, 2000. **875**(1-2): p. 23-34.

86. Lee, M.G., O.K. Hassani, and B.E. Jones, *Discharge of identified orexin/hypocretin neurons across the sleep-waking cycle.* J Neurosci, 2005. **25**(28): p. 6716-20.

87. Aston-Jones, G., C. Chiang, and T. Alexinsky, *Discharge of noradrenergic locus coeruleus neurons in behaving rats and monkeys suggests a role in vigilance.* Prog Brain Res, 1991. **88**: p. 501-20.

88. Nambu, T., et al., *Distribution of orexin neurons in the adult rat brain.* Brain Res, 1999. **827**(1-2): p. 243-60.

89. McGinty, D.J. and R.M. Harper, *Dorsal raphe neurons: depression of firing during sleep in cats.* Brain Res, 1976. **101**(3): p. 569-75.

90. Sakai, K. and S. Crochet, *Role of dorsal raphe neurons in paradoxical sleep generation in the cat: no evidence for a serotonergic mechanism.* Eur J Neurosci, 2001. **13**(1): p. 103-12.

91. Mallick, B.N., et al., *Role of norepinephrine in the regulation of rapid eye movement sleep.* J Biosci, 2002. **27**(5): p. 539-51.

92. Wikipedia, *definition of limit cycle.*

93. Edelstein-Keshet, L., *Chapter8 Limit Cycles, Oscillations, and Excitable Systems.* Mathematical Models in Biology, 2005: p. 311-379.

94. C.Lewis, D., *A Qualitative Analysis of S-System: Hopf Bifurcations.* Canonical Nonlinear Modeling. S-System Approach to Understanding Complexity, 1991: p. 304-344.

95. Xi, M.C., F.R. Morales, and M.H. Chase, *Effects on sleep and wakefulness of the injection of hypocretin-1 (orexin-A) into the laterodorsal tegmental nucleus of the cat.* Brain Res, 2001. **901**(1-2): p. 259-64.

96. Verret, L., et al., *Localization of the neurons active during paradoxical (REM) sleep and projecting to the locus coeruleus noradrenergic neurons in the rat.* J Comp Neurol, 2006. **495**(5): p. 573-86.

97. Sakai, K. and Y. Koyama, *Are there cholinergic and non-cholinergic paradoxical sleep-on neurones in the pons?* Neuroreport, 1996. **7**(15-17): p. 2449-53.

98. Shouse, M.N. and J.M. Siegel, *Pontine regulation of REM sleep components in cats: integrity of the pedunculopontine tegmentum (PPT) is important for phasic events but unnecessary for atonia during REM sleep.* Brain Res, 1992. **571**(1): p. 50-63.

99. Sakai, K. and S. Crochet, *A neural mechanism of sleep and wakefulness.* sleep biol rhythms, 2003. **1**: p. 29-43.

100. Koyama, Y. and K. Sakai, *Modulation of presumed cholinergic mesopontine tegmental neurons by acetylcholine and monoamines applied iontophoretically in unanesthetized cats.* Neuroscience, 2000. **96**(4): p. 723-33.

101. Takahashi, K., et al., *Effects of orexin on the laterodorsal tegmental neurones.* Psychiatry Clin Neurosci, 2002. **56**(3): p. 335-6.

102. Mesulam, M.M., et al., *Central cholinergic pathways in the rat: an overview based on an alternative nomenclature (Ch1-Ch6).* Neuroscience, 1983. **10**(4): p. 1185-201.

103. Gritti, I., et al., *GABAergic and other noncholinergic basal forebrain neurons, together with cholinergic neurons, project to the mesocortex and isocortex in the rat.* J Comp Neurol, 1997. **383**(2): p. 163-77.

104. Gritti, I., L. Mainville, and B.E. Jones, *Projections of GABAergic and cholinergic basal forebrain and GABAergic preoptic-anterior hypothalamic neurons to the posterior lateral hypothalamus of the rat.* J Comp Neurol, 1994. **339**(2): p. 251-68.

105. Zaborszky, L. and A. Duque, *Local synaptic connections of basal forebrain neurons.* Behav Brain Res, 2000. **115**(2): p. 143-58.

106. Lee, M.G., et al., *Sleep-wake related discharge properties of basal forebrain neurons recorded with micropipettes in head-fixed rats.* J Neurophysiol, 2004. **92**(2): p. 1182-98.

107. Manns, I.D., A. Alonso, and B.E. Jones, *Discharge properties of juxtacellularly labeled and immunohistochemically identified cholinergic basal forebrain neurons recorded in association with the electroencephalogram in anesthetized rats.* J Neurosci, 2000. **20**(4): p. 1505-18.

108. Manns, I.D., A. Alonso, and B.E. Jones, *Rhythmically discharging basal forebrain units comprise cholinergic, GABAergic, and putative glutamatergic cells.* J Neurophysiol, 2003. **89**(2): p. 1057-66.

109. Gaus, S.E., et al., *Ventrolateral preoptic nucleus contains sleep-active, galaninergic neurons in multiple mammalian species.* Neuroscience, 2002. **115**(1): p. 285-94.

110. Steininger, T.L., et al., *Subregional organization of preoptic area/anterior hypothalamic projections to arousal-related monoaminergic cell groups.* J Comp Neurol, 2001. **429**(4): p. 638-53.

111. Gvilia, I., et al., *Homeostatic regulation of sleep: a role for preoptic area neurons.* J Neurosci, 2006. **26**(37): p. 9426-33.

112. Gvilia, I., et al., *Preoptic area neurons and the homeostatic regulation of rapid eye movement sleep.* J Neurosci, 2006. **26**(11): p. 3037-44.

113. Suntsova, N., et al., *The median preoptic nucleus reciprocally modulates activity of arousal-related and sleep-related neurons in the perifornical lateral hypothalamus.* J Neurosci, 2007. **27**(7): p. 1616-30.